SURFACE WAVE PROPAGATION THROUGH ANISOTROPIC CIRCULAR, CYLINDRICAL DIELECTRIC ROD WAVEGUIDE*

D. K. PAUL

(Department of Electrical Communication Enginecring, Indian Institute of Science, Bangalore-12, India)

(Received on October 22, 1965)

ABSTRACT

The expressions for the propagation characteristics, such as, thc radial propagation constants (K), the axial propagation constant (γ), the guided wavelength (λ_g), and the cut-off conditions for a circular, cylindrical, anisotropic dielectric rod waveguide excited by the symmetric electric (TM_{01}) and symmetric magnetic (TE_{01}) modes have been derived. Numerical calculation of these characteristics (K, γ, λ_g) as a function of the diameter (d) and the dielectri cconstant (ϵ_1) of the guide have been completed and the results are presented graphically. The eleetric and the magnetic field distributions inside and outside the waveguide as a function of a diameter (d) are also given.

1. INTROUCTION

The propagation characteristics of surface waves on different structures have been discussed in an illuminating manner by Barlow and Brown (1962) and others. Several authors have studied the surface wave structures in the form of corrugated, circular, cylindrical guide. Barlow and Karbowiak (1954) did the experimental investigations of surface waves on corrugated, circular, cylindrical metal rods. Simon and Weill (1952) have used a limiting form of the corrugated conducting cylinder excited in the dipole mode, consisting of an array of conducting disks normal to the axis and spaced at regular, periodic intervals. Piefke (1959) has studied the corrugated structure excited in the HE_{11} mode. The object of this paper is to present the theoretical investigations on the propagation of microwaves through an anisotropic dielectric rod waveguide excited in TE_{01} and TM_{01} modes

2. FIELD COMPONENTS

The field components inside and outside the waveguide (Figure I) when excited in the TE_{01} and TM_{01} modes have been derived from the Maxwell's

---

* My attention has been drawn to a previous paper on the same subject by P. R. Longaker appearing in IEEE Transactions on MTT, Vol. 11, November 1963. I wish to state that I was aware of this particular paper in question and I havc corresponded with Dr. Longaker wherein I had pointed out certain discrepancies in his paper, which have been acknowledged by him. In view of this, this previous publication does not in any way detract the value of this communication.

Equations by solving the wave equation and are given below. A harmonic time dependence of the field components has been assumed and is omitted in the expressions for the sake of convenience. The anisotropic dielectric rod waveguide and the surrounding medium (Figure 1), are assumed to be lossless and have the same permeability, μ. Therefore, the propagation constant, $\gamma - i\beta = i2\pi/\lambda_g$, λ_g being the wavelength of the guided wave. The dielectric constant, ϵ_1, of the waveguide is a tensor and is represented as follows,

$$\epsilon_1 = \begin{Bmatrix} \epsilon_\rho & 0 & 0 \\ 0 & \epsilon_\rho & 0 \\ 0 & 0 & \epsilon_z \end{Bmatrix} \qquad [1]$$

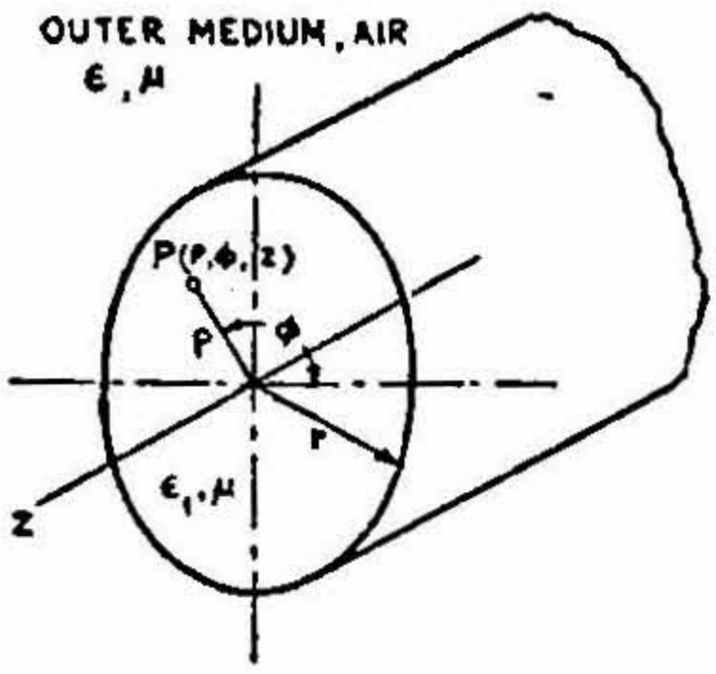

FIG. I

The Co-ordinate system (ρ, ϕ, z) in the anisotropic dielectric rod wave-guide

2.1 TE_{01} – *Mode*

Inside the waveguide, $\rho < r$, radius of the guide,

$$H_{z1} = A\, J_o(K_1^E \rho) \exp(-\gamma_1^E z)$$

$$H_{\rho 1} = iA\,[\bar{\epsilon}_\rho (\lambda_g/\lambda_0)^2 - 1]^{-\frac{1}{2}}\, J_1(K_1^E \rho)\,.\,\exp.\,(-\gamma_1^E z) \qquad [2]$$

$$E_{\phi 1} = -iA\,[\mu/\epsilon]^{\frac{1}{2}}\,[\bar{\epsilon}_\rho - (\lambda_0/\lambda_g)^2]^{-\frac{1}{2}}\, J_1(K_1^E \rho)\,.\,\exp.\,(-\gamma_1^E z)$$

Outside the waveguide, $\rho > r$,

$$H_{z2} = BH_0^{(1)}(K_2^E \rho)\,.\exp(-\gamma_2^E z)$$

$$H_{\rho 2} = iB\,[\lambda_g/\lambda_0)^2 - 1]^{-\frac{1}{2}}\, H_1^{(1)}(K_2^E \rho)\,.\,\exp.\,(-\gamma_2^E z) \qquad [3]$$

$$E_{\phi 2} = -iB\,[\mu/\epsilon]^{\frac{1}{2}}\,[1 - (\lambda_0/\lambda_g)^2]^{-\frac{1}{2}}\, H_1^{(1)}(K_2^E \rho)\,.\,\exp.\,(-\gamma_2^E z)$$

The variation of γ_1^E and γ_2^E in the axial direction is considered as

$$\exp.\,(-\gamma^E z).$$

2.2 TM_{01} – *Mode*

Inside the waveguide, $\rho < r$,

$$E_{z1} = C\, J_0 (K_1^H \rho) . \exp (-\gamma_1^H z)$$

$$E\rho_1 = iC [\bar{\epsilon}_z/\bar{\epsilon}_\rho] [\bar{\epsilon}_z (\lambda_g/\lambda_0)^2 - \bar{\epsilon}_z/\bar{\epsilon}_\rho]^{-\frac{1}{2}} J_1 (K_1^H \rho) . \exp. (-\gamma_1^H z) \quad [4]$$

$$H_{\phi 1} = iC\, \bar{\epsilon}_z [\epsilon/\mu]^{\frac{1}{2}} [\bar{\epsilon}_z - (\lambda_0/\lambda_g)^2 . (\bar{\epsilon}_z/\bar{\epsilon}_\rho)]^{-\frac{1}{2}} J_1 (K_1^H \rho) . \exp. (-\gamma_1^H z)$$

Outside the waveguide, $\rho > r$,

$$E_{z2} = D H_0^{(1)} (K_2^H \rho) . \exp. (-\gamma_2^H z)$$

$$E_{\rho 2} = i\, D [(\lambda_g/\lambda_0)^2 - 1]^{-\frac{1}{2}} H_1^{(1)} (K_2^H \rho) . \exp. (-\gamma_2^H z) \quad [5]$$

$$H_{\phi 2} = i\, D [\epsilon/\mu]^{\frac{1}{2}} [1 - (\lambda_0/\lambda_g)^2]^{-\frac{1}{2}} H_1^{(1)} (K_2^H \rho) . \exp. (-\gamma_2^H z)$$

The variation of γ_1^H and γ_2^H in the axial direction is considered as $\exp. (-\gamma^H z)$.

In the equations (2) to (5)

K_1^E = Radial propagation constant inside the guide for *TE* mode

$$= [(\gamma_1^E)^2 + \omega^2 \mu \epsilon_\rho]^{\frac{1}{2}} = (2\pi/\lambda_0) [\bar{\epsilon_\rho} - (\lambda_0/\lambda_g)^2]^{\frac{1}{2}} \quad [6]$$

K_1^H = Radial propagation constant inside the guide for *TM* mode

$$= [\{\gamma_1^H)^2 + \omega^2 \mu \epsilon_\rho\} (\bar{\epsilon}_z/\bar{\epsilon}_\rho)]^{\frac{1}{2}} = (2\pi/\lambda_0) [\bar{\epsilon}_z - (\lambda_0/\lambda_g)^2 (\bar{\epsilon}_z/\bar{\epsilon}_\rho)]^{\frac{1}{2}} \quad [7]$$

K_2 = Radial propagation constant outside the waveguide

$$= [\gamma^2 + \omega^2 \mu \epsilon]^{\frac{1}{2}} = (2\pi/\lambda_0) \quad [1 - (\lambda_0/\lambda_g)^2]^{\frac{1}{2}} \quad [8]$$

$$\bar{\epsilon}_z = [\epsilon_z/\epsilon] , \bar{\epsilon}_\rho = [\epsilon_\rho/\epsilon] \quad [9]$$

3. Characteristic Equations

The characteristic equations for both the modes as obtained by matching the field components at the boundary surface, $\rho = r$, are given as follows :

3.1 TE_{01} *Mode*

$$x_1 \frac{J_0 (x_1)}{J_1 (x_1)} = x_2 \frac{H_0^{(1)} (x_2)}{H_1^{(1)} (x_2)} \quad [10]$$

Where, $x_1 = K_1^E r$ and $x_2 = K_2^E r$ [11]

From equations (6) and (8), we have

$$[x_1^2 + (x_2/i)^2] = (\pi d/\lambda_0)^2 [\bar{\epsilon}_\rho - 1] \qquad [12]$$

3.2 *TM_{01} Mode*

$$y_1 \frac{J_0(y_1)}{J_1(y_1)} = \bar{\epsilon}_z y_2 \frac{H_0^{(1)}(y_2)}{H_1^{(1)}(y_2)} \qquad [13]$$

where, $y_1 = K_1^H r$ and $y_2 = K_2^H r$ [14]

From equations [7] and [8], we have,

$$[y^2 + y_2/i)^2 (\bar{\epsilon}_z/\bar{\epsilon}_\rho)] = (\pi d/\lambda_0)^2 [\bar{\epsilon}_z - (\bar{\epsilon}_z/\bar{\epsilon}_\rho)] \qquad [15]$$

4. Solution of the Characteristic Equations

In solving these equations, we assume that there is no dielectric loss. Thus, γ^2 and hence K_1^2 will be real. To have a non-radiating mode, the arguments of the Hankel functions must be imaginary. Therefore, K_2 must be imaginary and so, K_1 is real. Now, given that K_1 is real and K_2 is imaginary, the characteristic equations are solved graphically.

4.1 *Guided Wavelength*

The expressions for the guided wavelength can be determined from the equations [6] and [8], and [7] and [8] for the *TE* and *TM* waves, respectively, and are given as follows:

(*a*) *TE_{01} Mode*:

From equations [6] and [8], we have on putting $x_1 = K_1^E r$ and $x_2 = K_2^E r$,

$$[\lambda_g/\lambda_0]^2 = [1 - (x_2 \lambda_0/\pi d)^2]^{-1} = [\bar{\epsilon}_\rho - (x_1 \lambda_0/\pi d)^2]^{-1} \qquad [16]$$

The results calculated as a function of (d/λ_0) and $\bar{\epsilon}_\rho$ are shown graphically in Figure II and Figure III, respectively.

(*b*) *TM_{01} Mode*:

From equations [7] and [8], we have on putting $y_1 = K_1^H r$ and $y_2 = K_2^H r$,

$$[\lambda_g/\lambda_0]^2 = [1 - (y_2 \lambda_0/\pi d)^2]^{-1} = [\bar{\epsilon}_z/\bar{\epsilon}_\rho][\bar{\epsilon}_z - (y_1 \lambda_0/\pi d)^2]^{-1} \qquad [17]$$

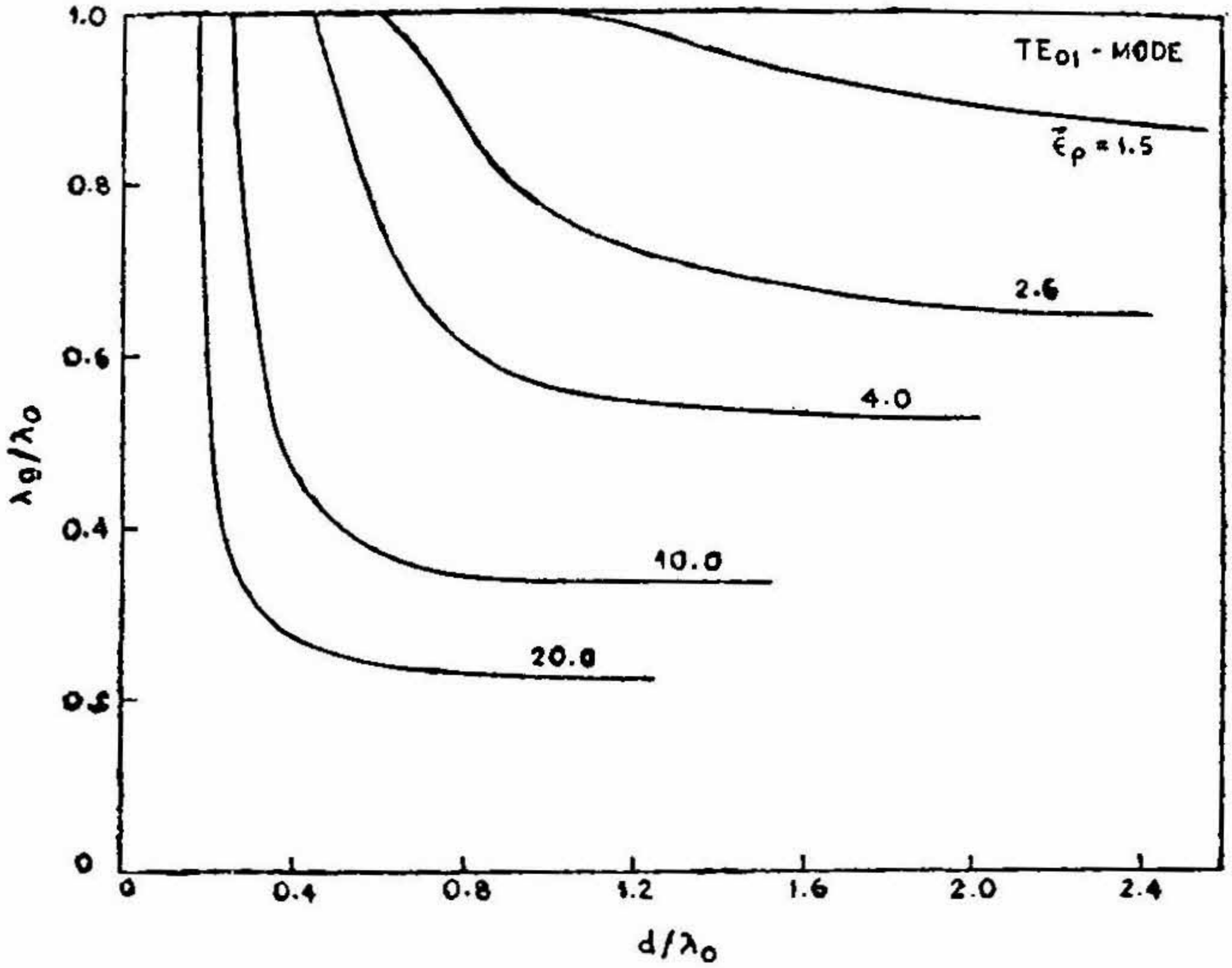

FIG. II

Variation of (λ_g/λ_0) with (d/λ_0) for TE_{01}—mode (λ_0=3.2 cms.)

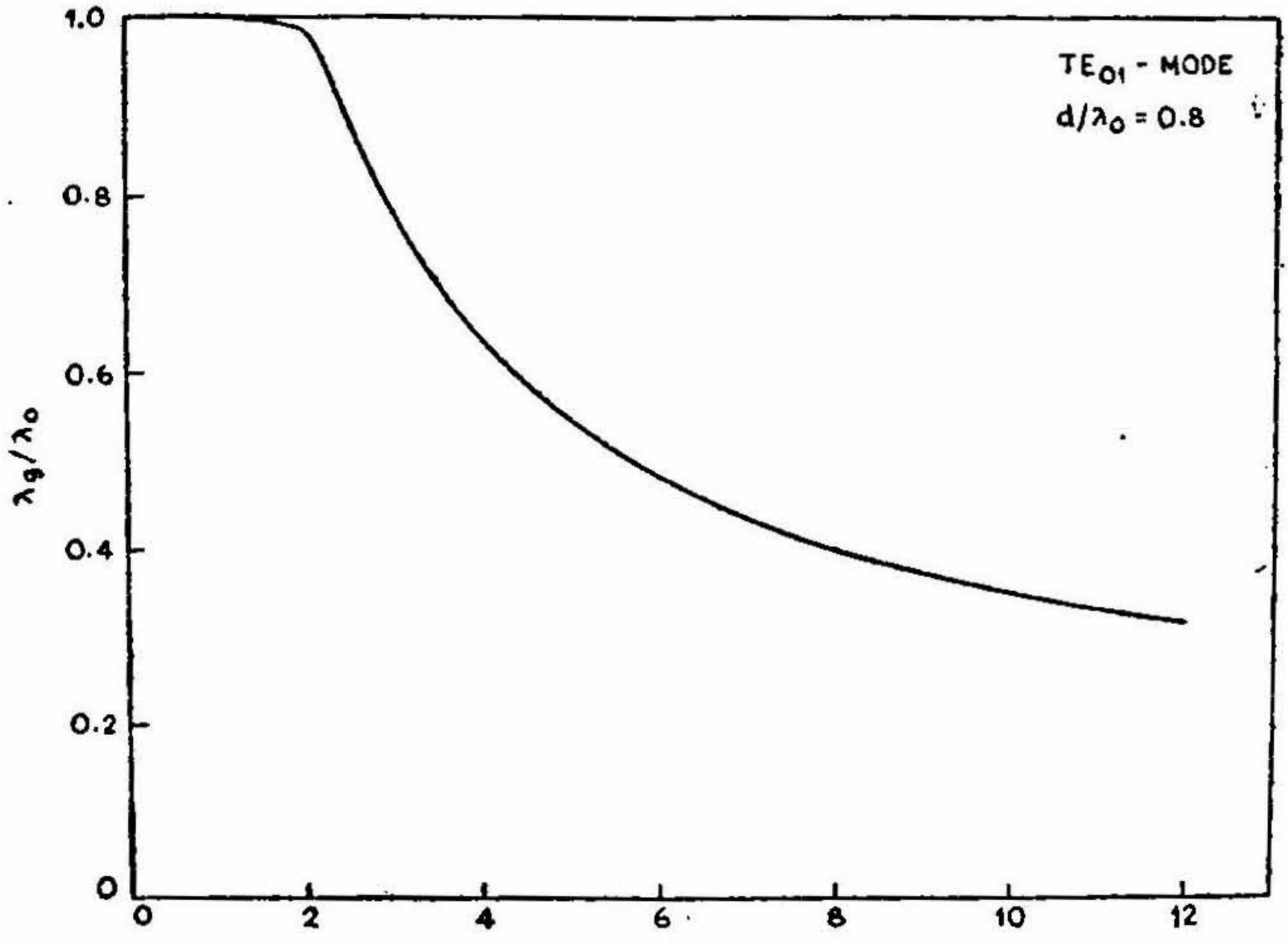

FIG. III

Variation of (λ_g/λ_0) with $\bar{\epsilon}_\rho$ for TE_{01}—mode (d/λ_0=0.8 and λ_0=3.2 cms.)

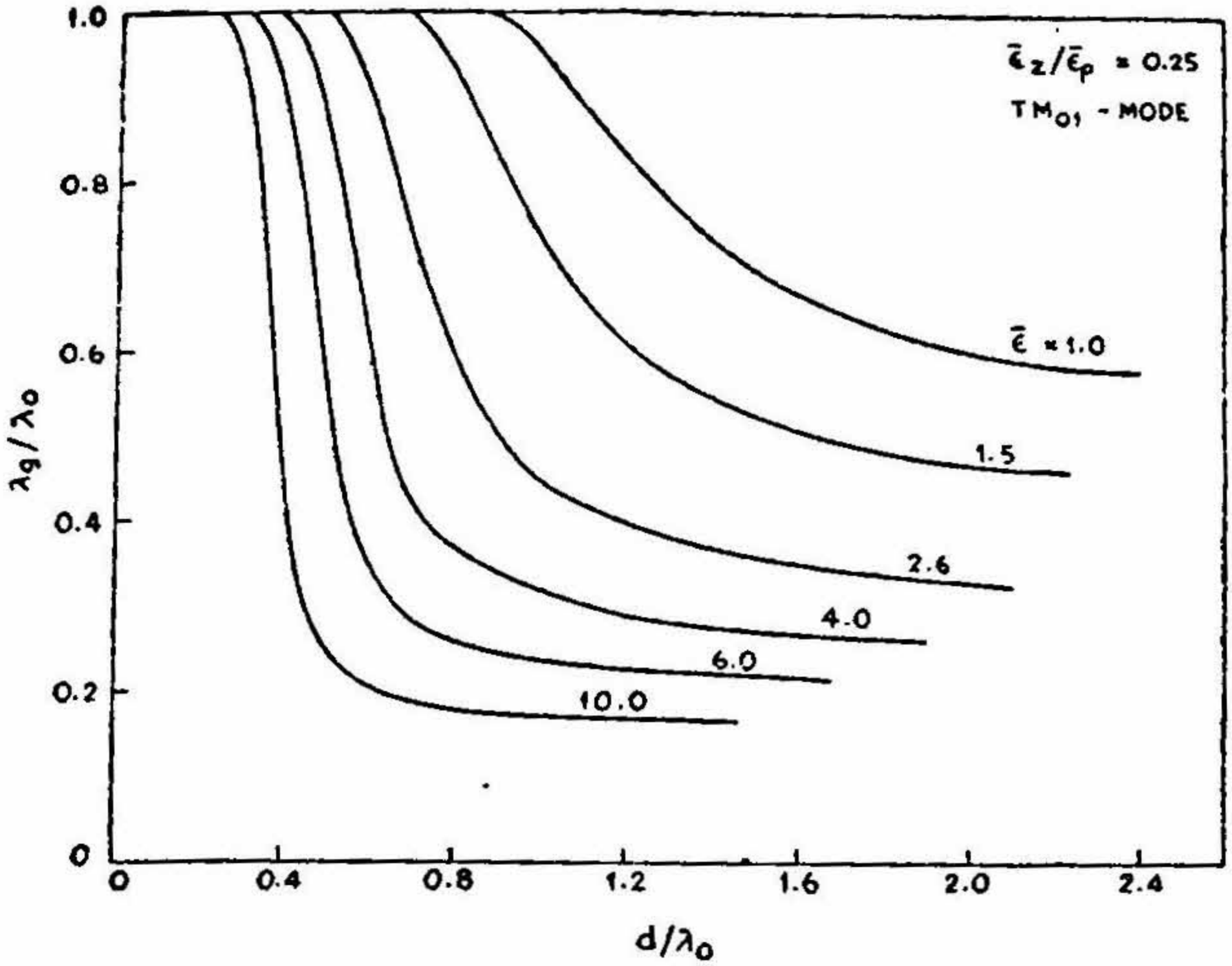

FIG. IV

Variation of (λ_g/λ_0) with (d/λ_0) for TM_{01}—mode (λ_0=3.2 cms. $\bar{\epsilon}_z/\bar{\epsilon}_\rho$ =0.25)

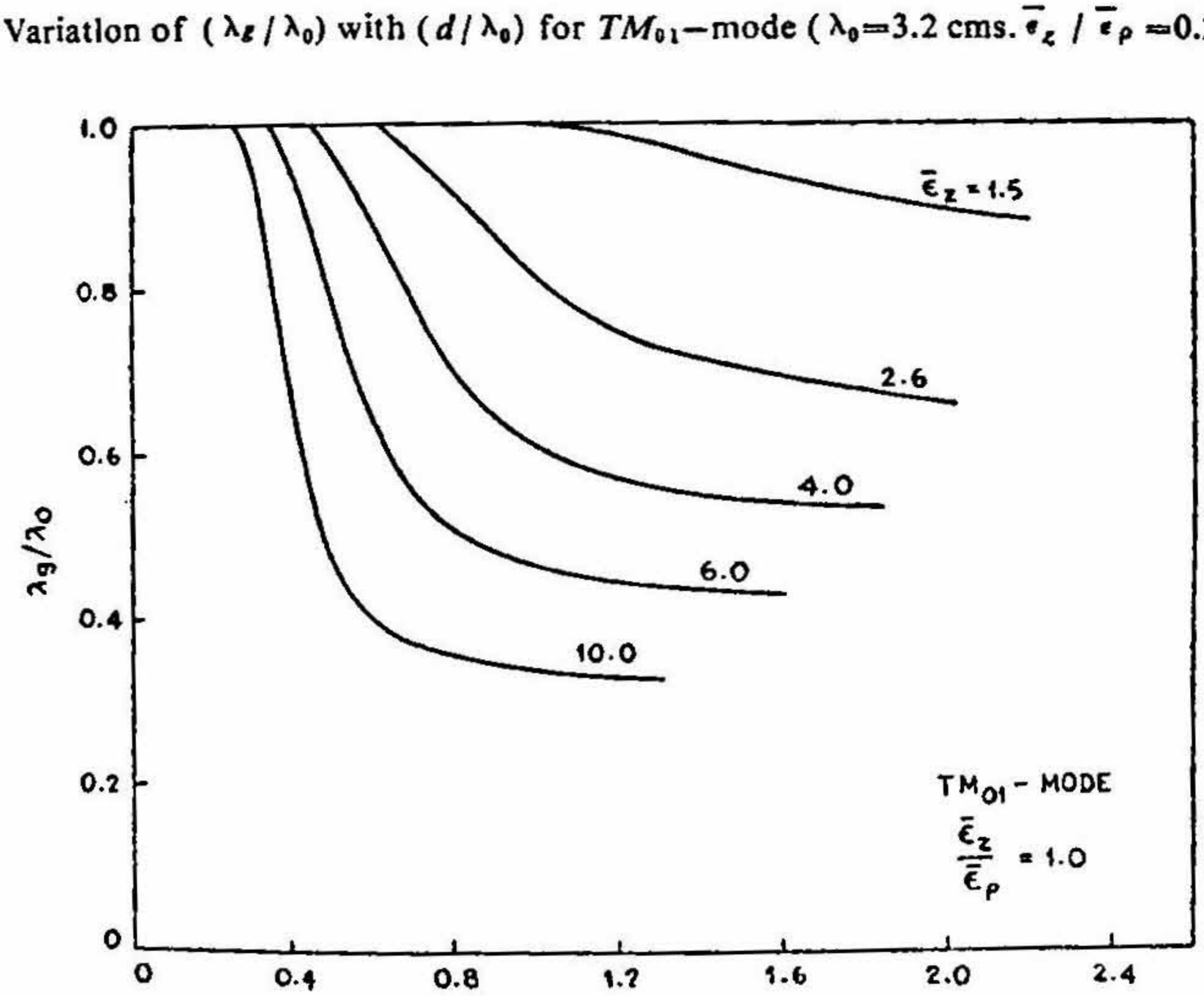

FIG. V

Variation of (λ_g/λ_0) with (d/λ_0) for TM_{01}—mode (λ_0=3.2 cms. $\bar{\epsilon}_z/\bar{\epsilon}_\rho$ = 1.0)

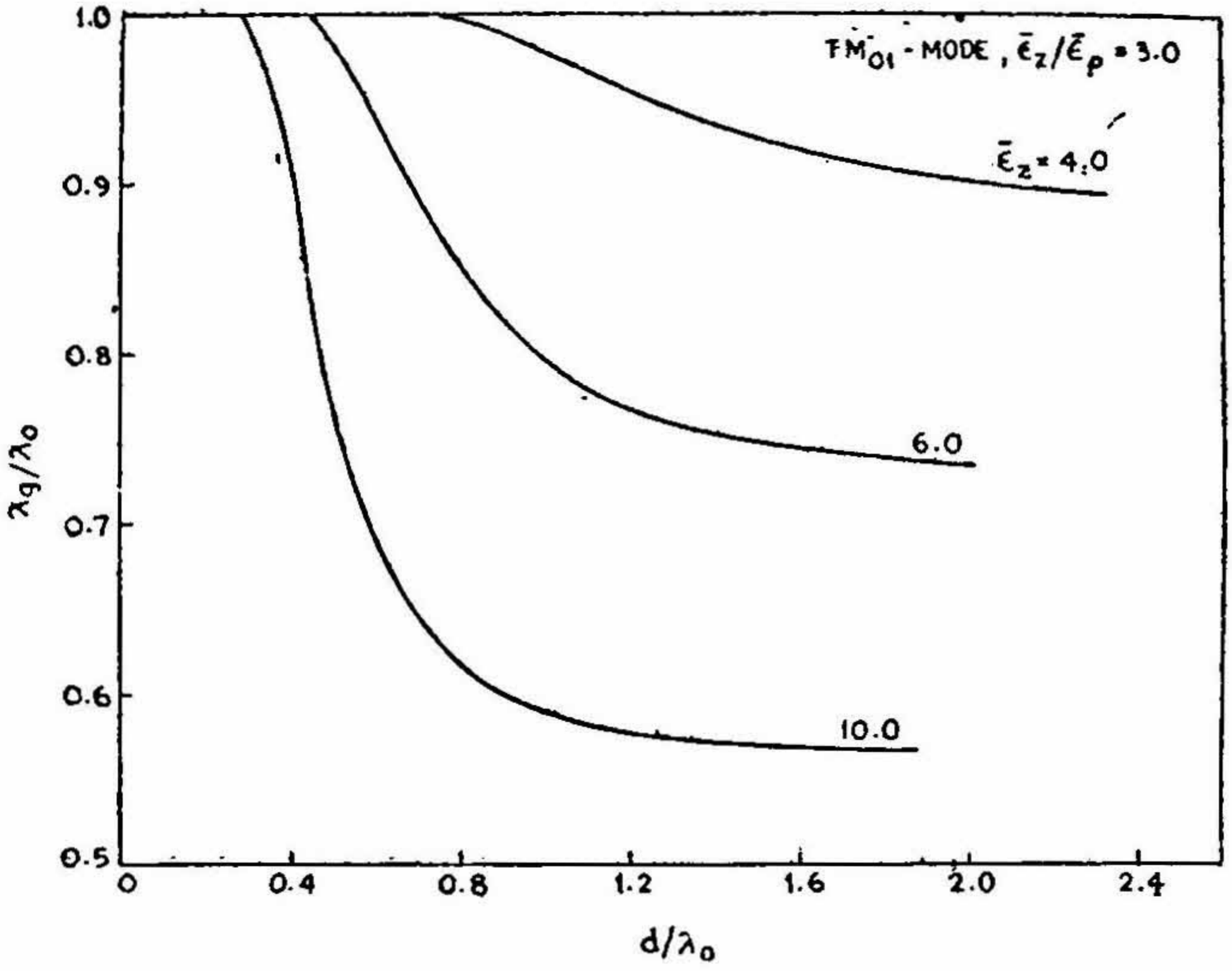

FIG. VI

Variation of (λ_g / λ_0) with (d / λ_0) for TM_{01}—mode (λ_0=3.2 cms. $\bar{\epsilon}_z / \bar{\epsilon}_\rho = 3.0$)

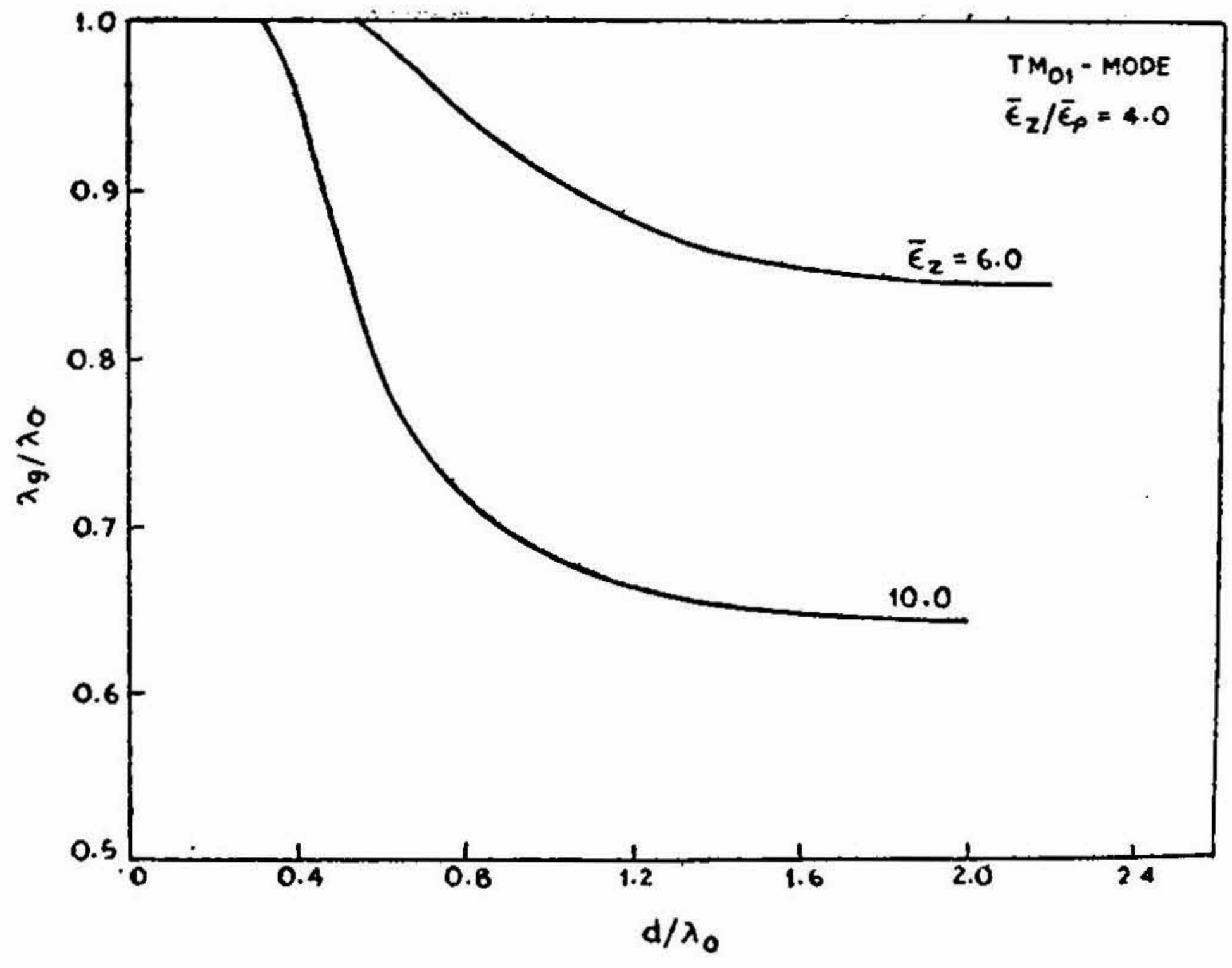

FIG. VII

Variation of (λ_g / λ_0) with (d / λ_0) for TM_{01}—mode (λ=3.2 cms. $\bar{e}_z / \bar{e}_\rho = 4.0$)

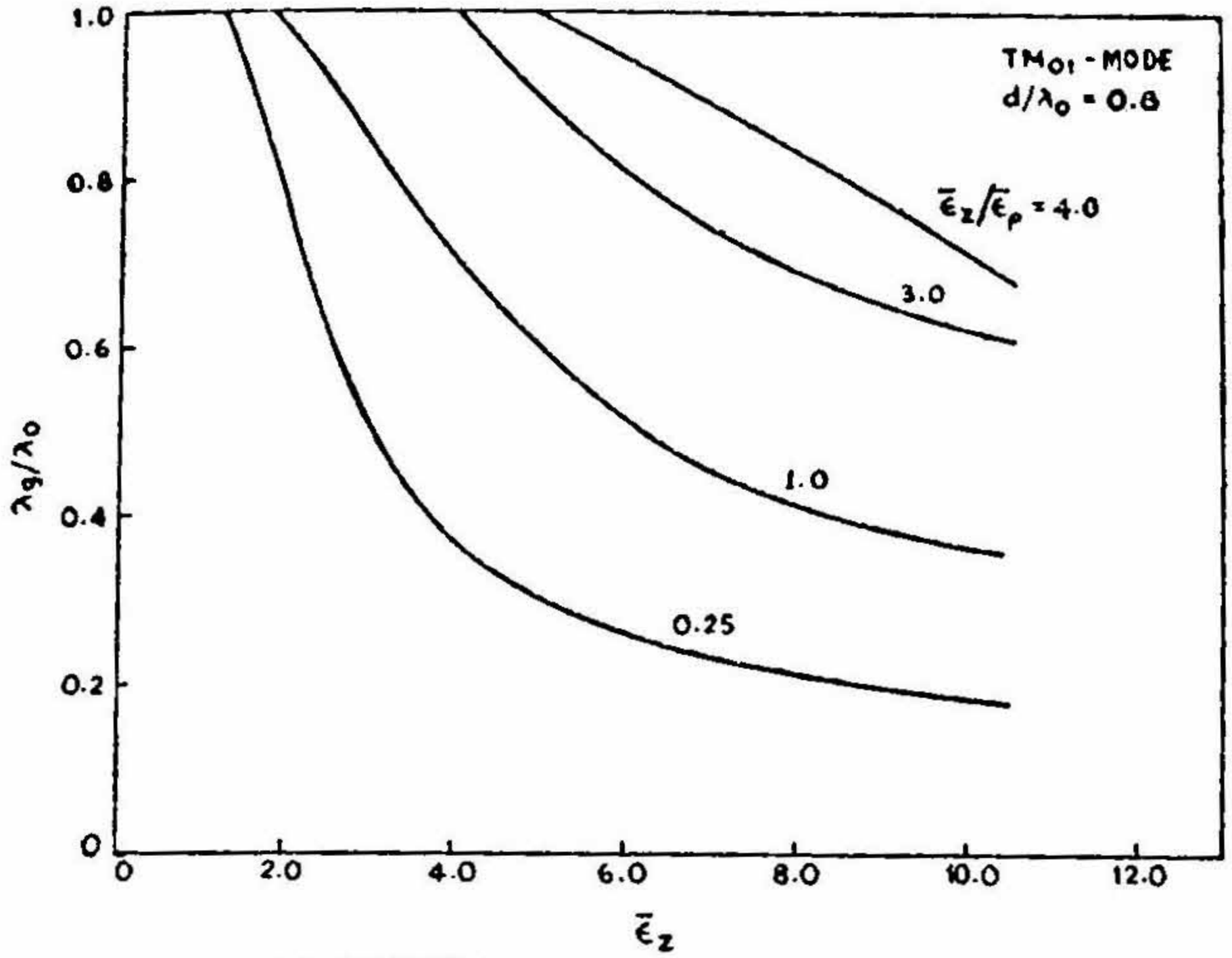

FIG. VIII

Variation of (λ_g/λ_0) with $\bar{\epsilon}_z$ for TM_{01}—mode $(d/\lambda_0 = 0.8,\ \lambda_0 = 3.2$ cms.)

These are calculated as a function of (d/λ_0) and $\bar{\epsilon}_z$ for different values of $[\bar{\epsilon}_z/\bar{\epsilon}_\rho]$ ranging from 0.25 to 4.0 and are shown graphically in Figures IV, V, VI, VII and VIII.

It will be seen, however, that for a dielectric medium of infinite extent, that is, (d/λ_0) tending to infinity, we have in the limiting case, $(\lambda_g/\lambda_0) = [\bar{\epsilon}_\rho]^{-\frac{1}{2}}$.

4.2 *Radial Propagation Constants*

The radial propagation constants (K_1 and K_2) are calculated from equations [11] and [14] for TE_{01} and TM_{01} modes, respectively. The variation of K_1 and K_2 as a function of (d/λ_0) for $\bar{\epsilon}_\rho = 1.5, 2.6, 4.0, 10.0, 20.0$ are plotted in Fig. IX and as a function of $\bar{\epsilon}_\rho$ with $(d/\lambda_0) = 0.8$ in Figure X for TE_{01} mode. For TM_{01} mode, these are plotted as a function of (d/λ_0) for $\epsilon_z = 1.0, 1.5, 2.6, 4,0, 6.0, 10.0$ with $[\bar{\epsilon}_z/\bar{\epsilon}_\rho]$ ranging from 0.25 to 4.0 in Figure XI, XII XIII and XIV and as a function of $\bar{\epsilon}_z$ for $(d/\lambda_0) = 0.8$ with $[\bar{\epsilon}_z/\bar{\epsilon}_\rho]$ ranging from 0.25 to 4.0 in Figure XV.

4.3 *Axial Propagation Constants*

The axial propagation constants (γ) are calculated from equations [6] and [7] for TE_{01} and TM_{01} modes, respectively. The variation of (γ/γ_0) with

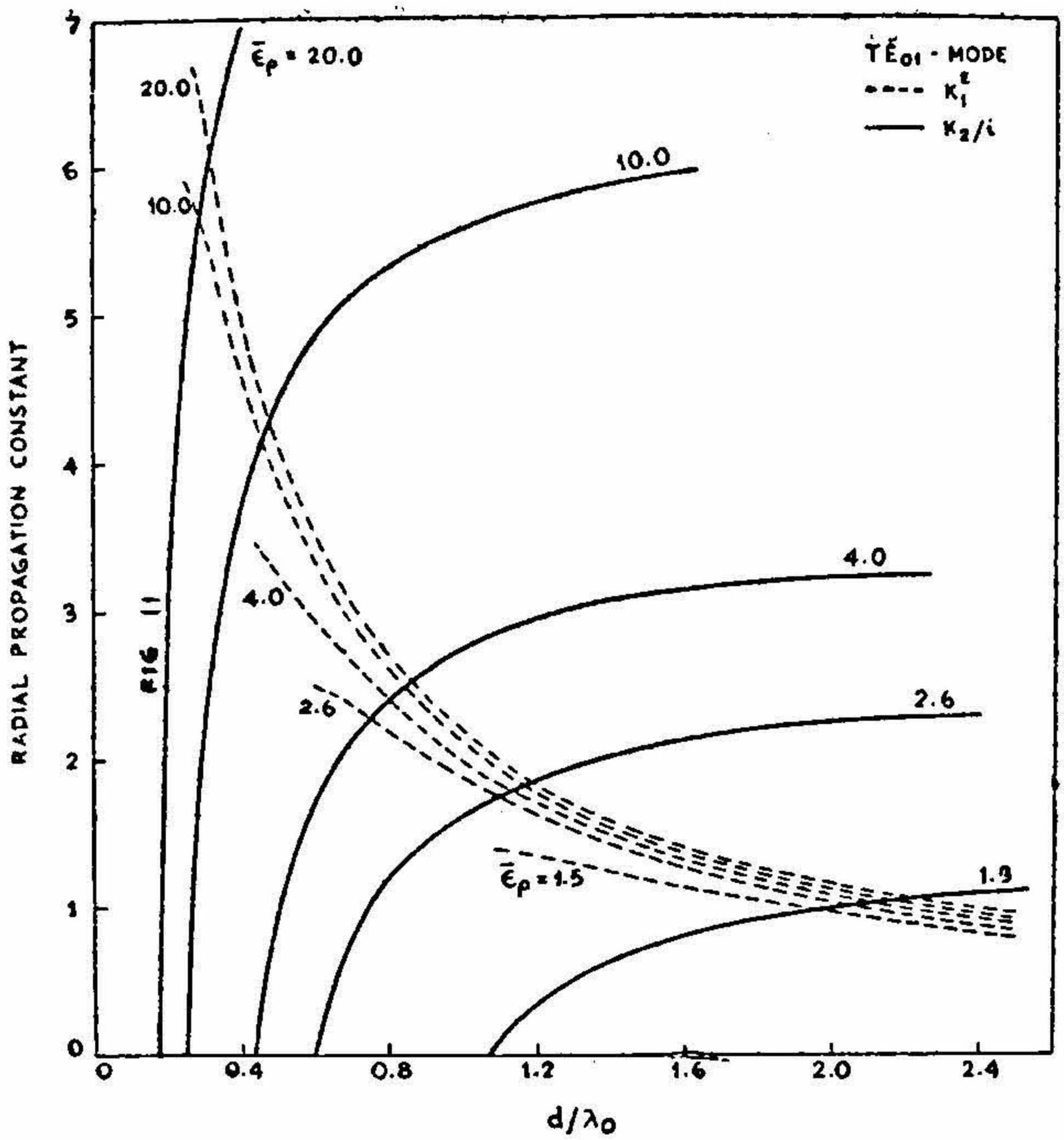

FIG. IX

Variation of the radial propagation eonstants, K_1^E and K_2^E with d/λ_0. (λ_0=3.2 cms.) for TE_{01} mode (As K_2 is imaginary K_2/i has been plotted)

respect to (d/λ_0) and $\bar{\epsilon}_\rho$ for TE_{01} mode are shown in Figures XVI and XVII, respectively. For TM_{01} mode, these are plotted as a function of (d/λ_0) for $\epsilon_z = 1.0$, 1.5, 2.6, 4.0, 6.0, 10.0 with $[\bar{\epsilon}_z/\bar{\epsilon}_\rho]$ ranging from 0.25 to 4.0 in Figures XVIII, XIX, XX and XXI and as a function of $\bar{\epsilon}_z$ for $(d/\lambda_0) = 0.8$ with $[\bar{\epsilon}_z/\bar{\epsilon}_\rho]$ ranging from 0.25 to 4.0 in Figure XXII.

4.4 *Field Configurations*

The electric and the magnetic field distributions inside and outside the anisotropic dielectric rod waveguide have been calculated from equations [2], [3], [4] and [5] for $(d/\lambda_0) = 0.8$. These are shown in in Figures XXIII, XXIV, XXV and in Figures XXVI, XXVII, XXVIII for TE_{01} and TM_{01} modes, respectively. The values of the field components have been normalised with respect to their values at the surface, $\rho = r$, of the guide.

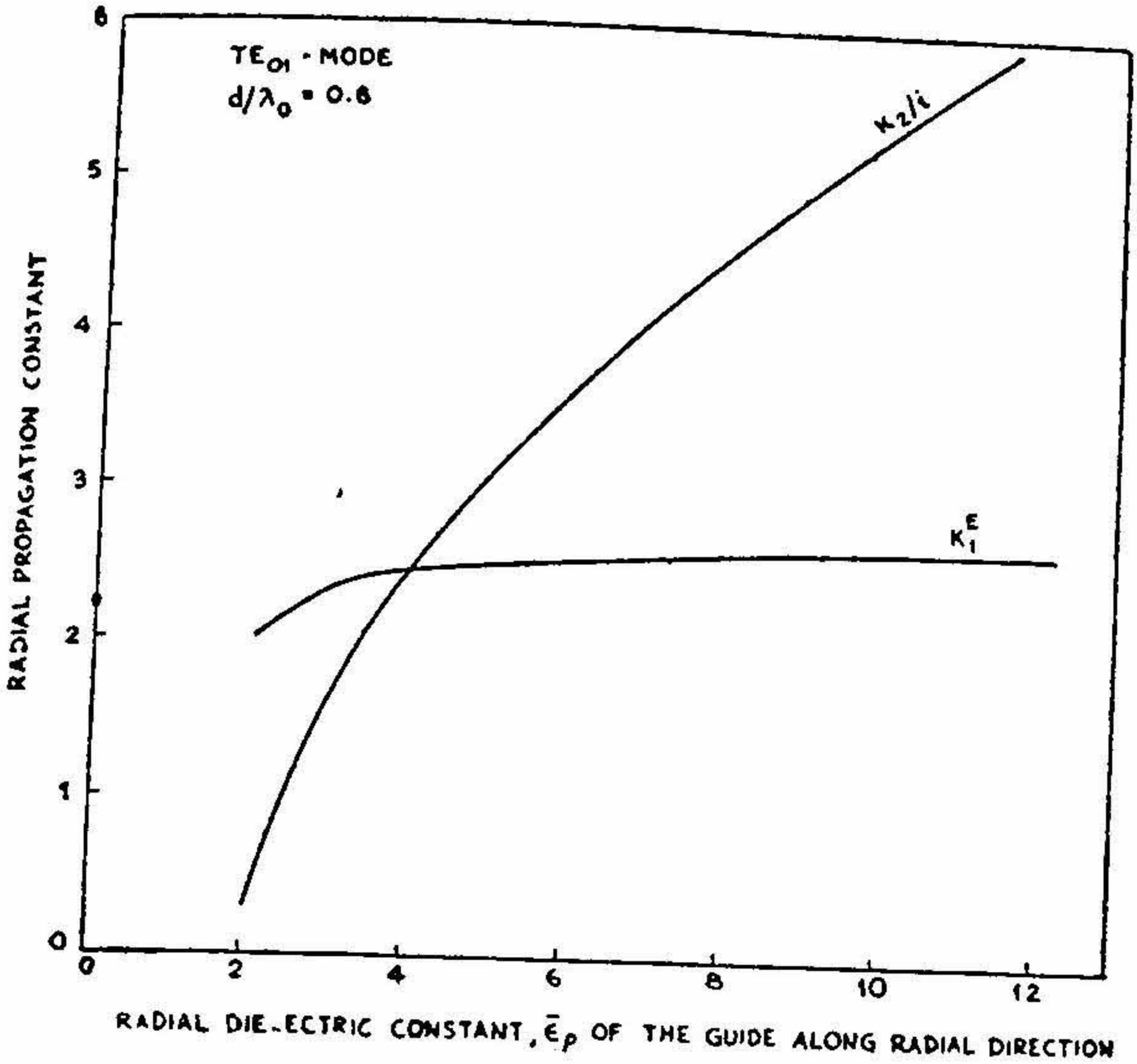

FIG. X

Variation of the radial propagation constants, K_1^E and K_2^E with $\bar{\epsilon}_\rho$ ($d/\lambda_0=0.8$, $\lambda_0=3.2$ cms.) for TE_{01}—mode

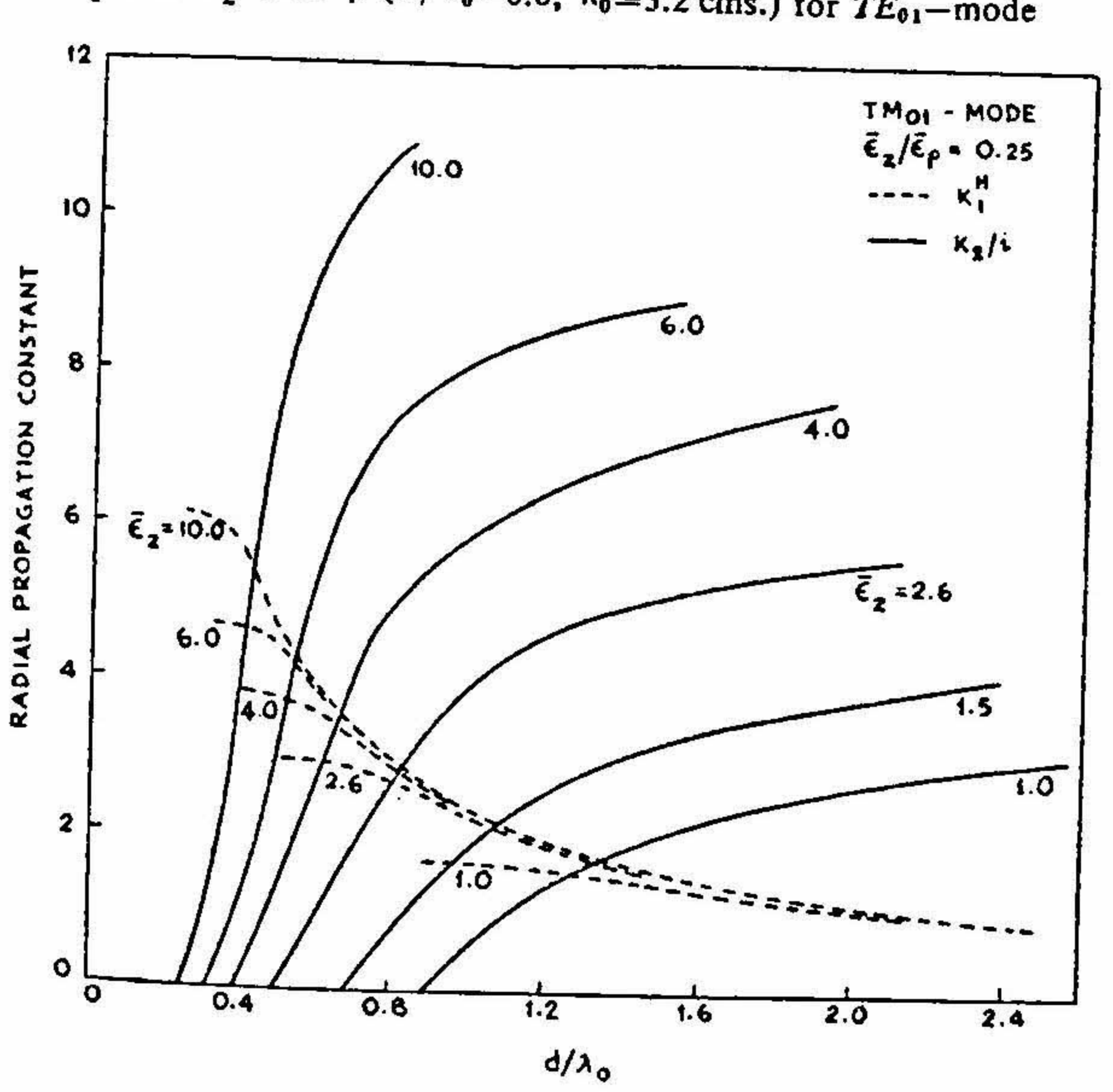

FIG. XI

Variation of the radial propagation constantants K_1^H and K_2^H with d/λ_0 ($\lambda_0=3.2$ cms. and $\bar{\epsilon}_z/\bar{\epsilon}_\rho=0.25$ for TM_{01}—mode

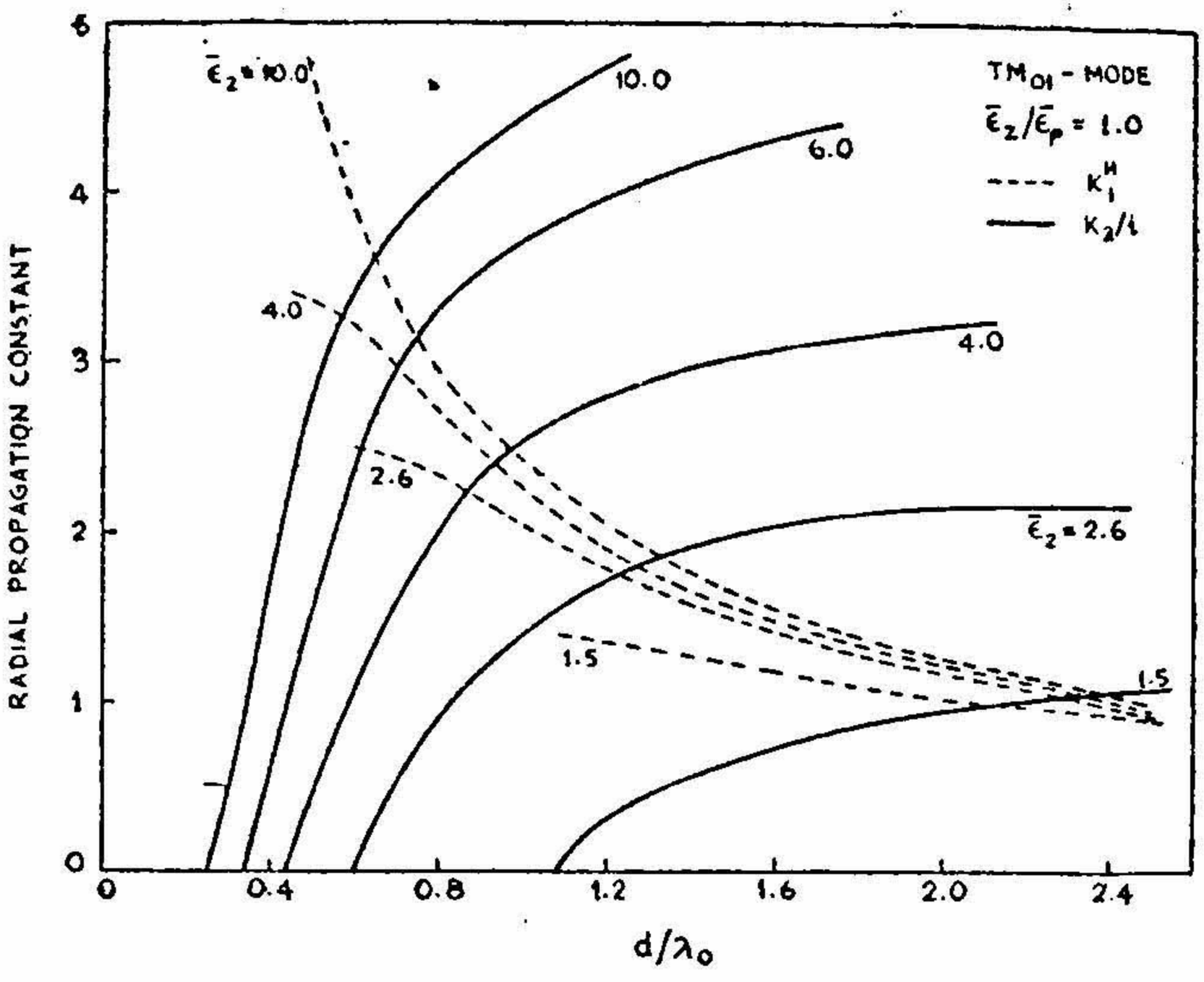

FIG. XII

Variation of the radial propagation constants, K_1^H and K_2^H with d/λ_0 (λ_0=3.2 cms. $\bar{\epsilon}_z / \bar{\epsilon}_\rho = 1.0$) for TM_{01}—mode

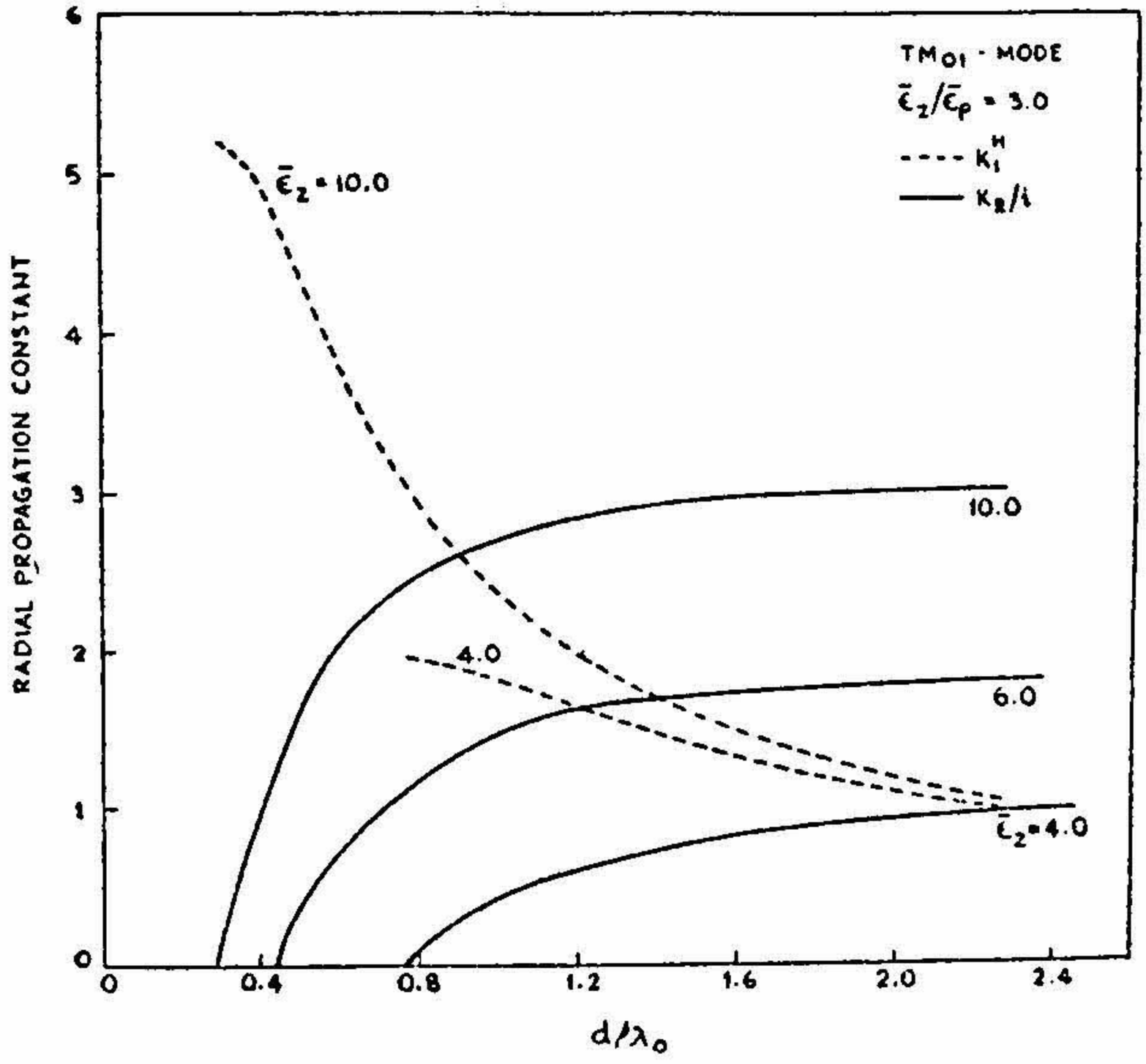

FIG. XIII

Variation of the radial propagation constants, K_1^H and K_2^H with d/λ_0 (λ_0=3.2 cms. $\bar{\epsilon}_z / \bar{\epsilon}_\rho = 3.0$) for TM_{01}—mode

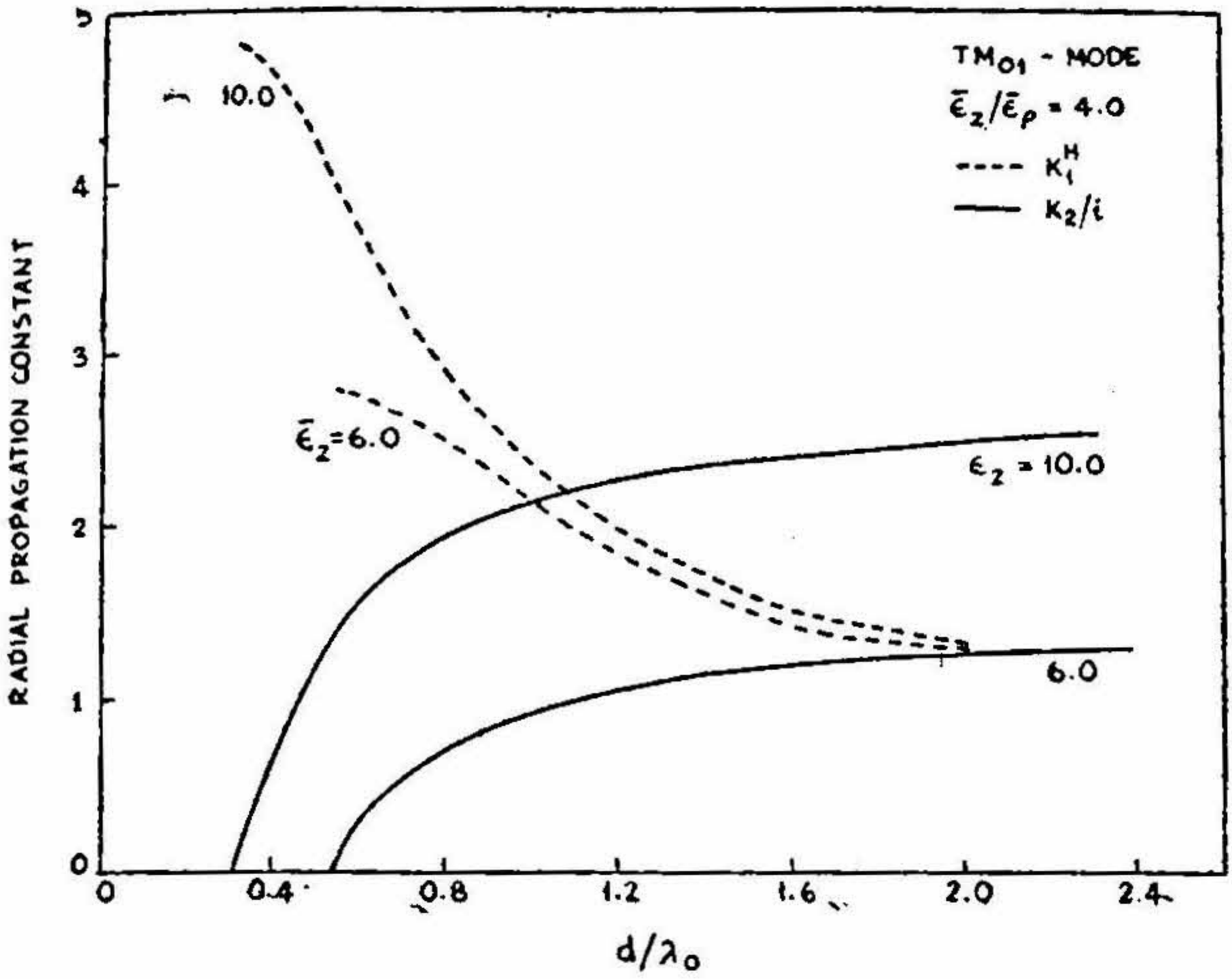

FIG. XIV

Variation of the radial propagation constants,
K_1^H and K_2^H with d/λ_0 (λ_0=3.2 cms. and $\bar{\epsilon}_z/\bar{\epsilon}_\rho = 4.0$) for TM_{01}—mode

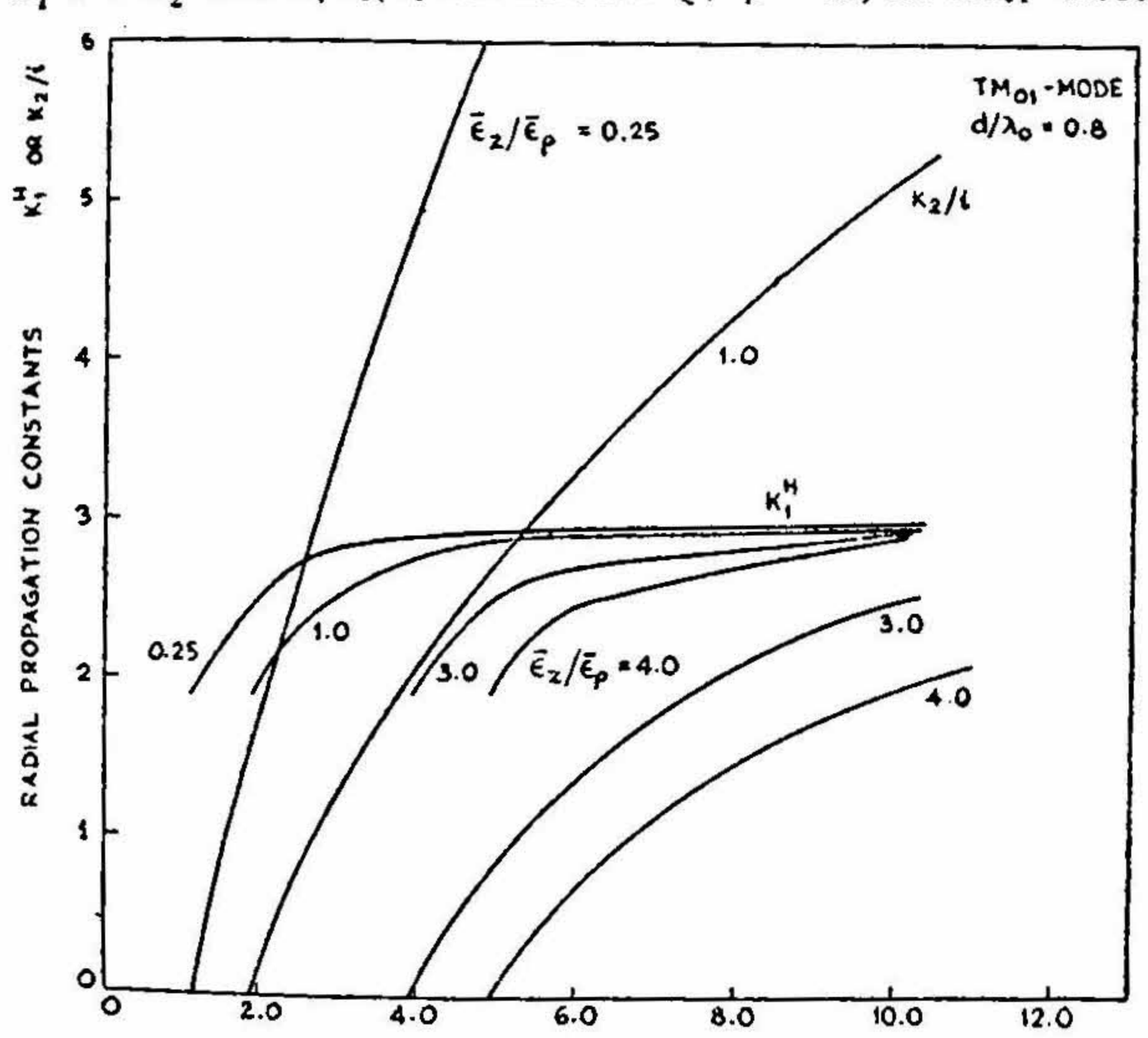

FIG. XV

Variation of the radial propagation constants
K_1^H and K_2^H with $\bar{\epsilon}_z$ (d/λ_0=0.8, λ_0=3.2 cms. for TM_{01}—mode)

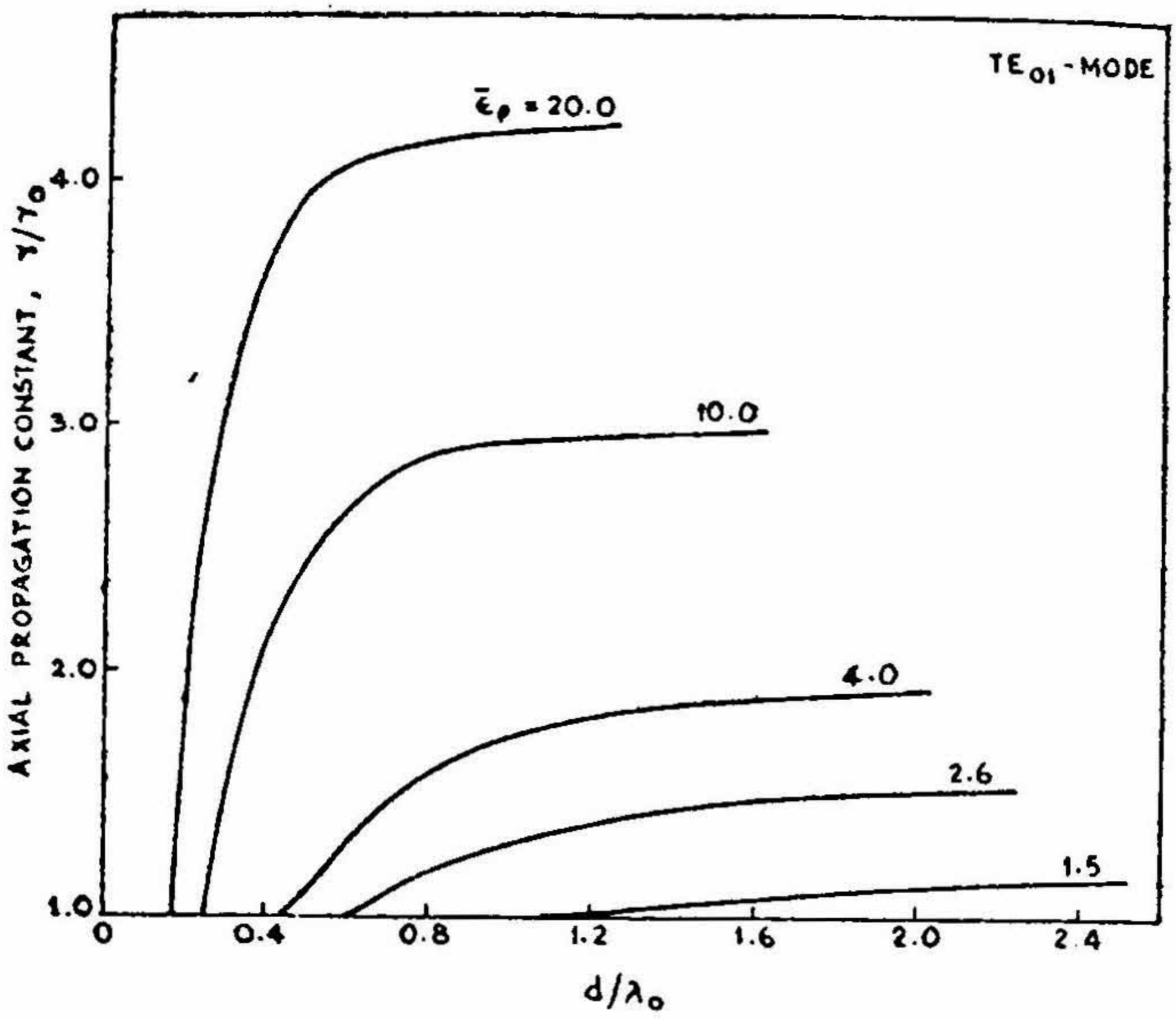

FIG. XVI

Variation of the axial propagation constants, γ^E / γ_0 with d / λ_0 (λ_0=3.2 cms.) for TE_{01}—mode

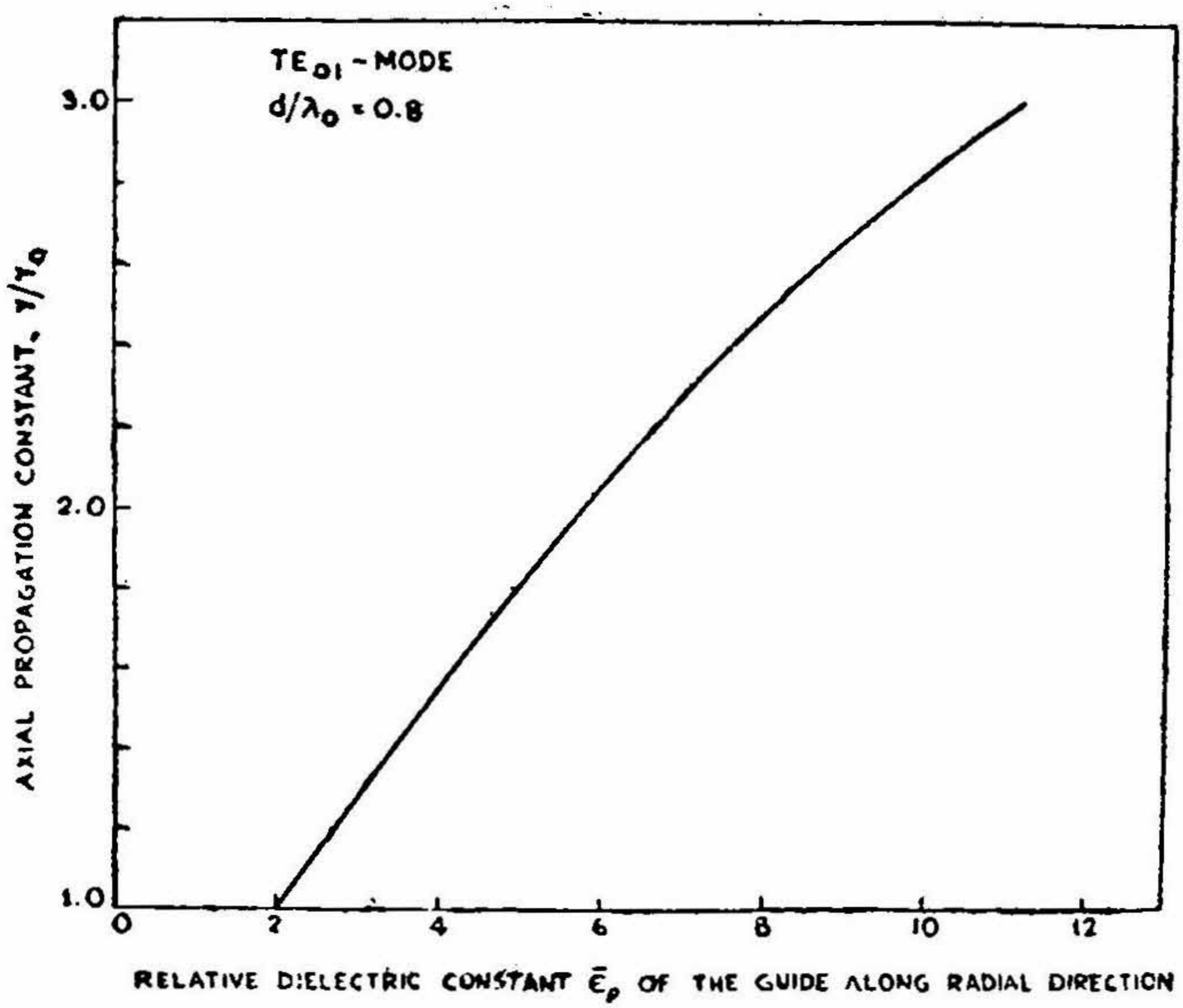

FIG. XVII

Variation of the axial propagation constant,
γ^E / γ_0 with $\bar{\epsilon}_\rho$, (d / λ=0.8, λ_0=3.2 cms.) for TE_{01}—mode

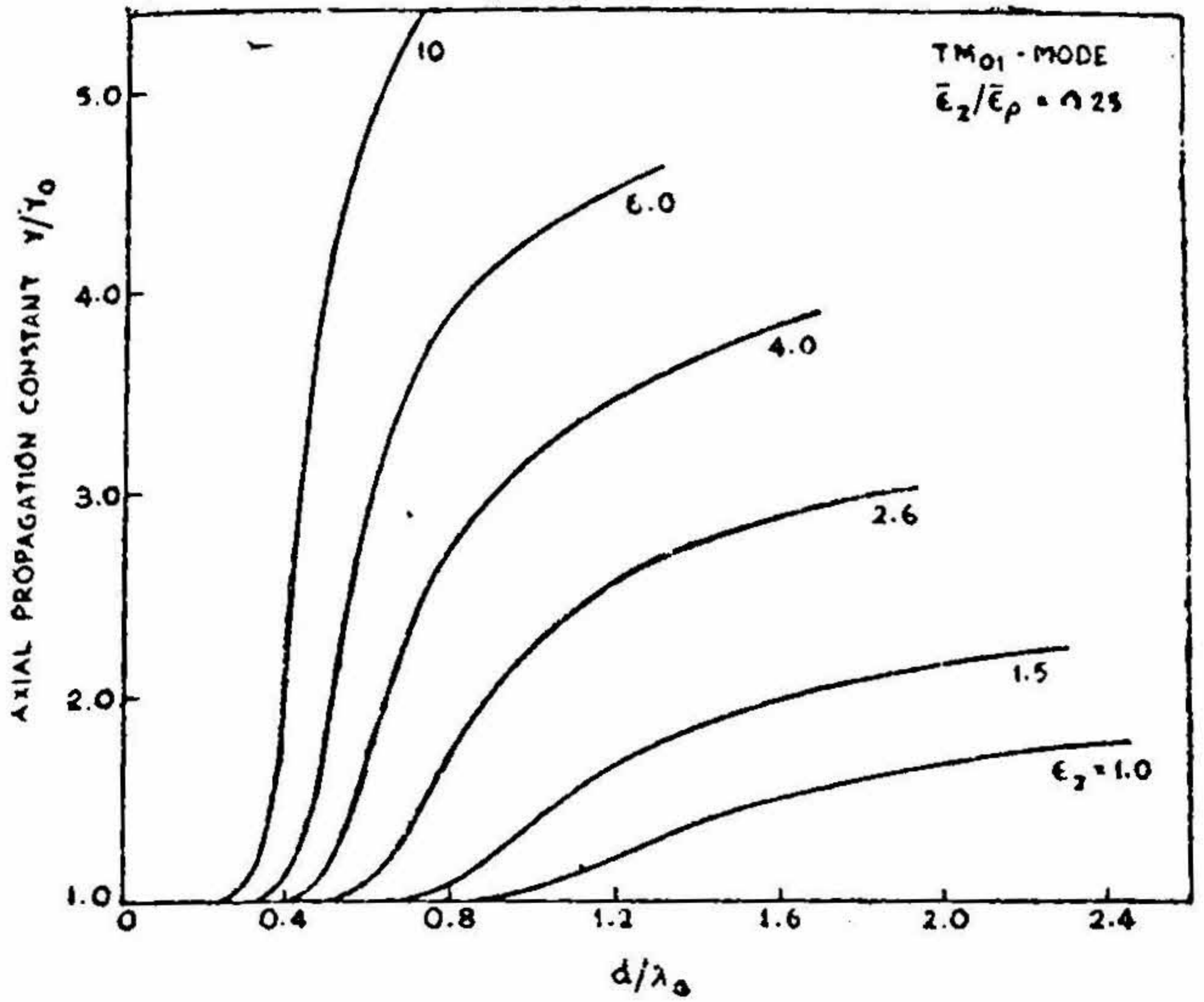

FIG. XVIII

Variation of the axial propagation constant,
$\gamma H / \gamma_0$ with d/λ_0 (λ_0=3.2 cms. $\bar{e}_z / \bar{e}_\rho = 0.25$) for TM_{01}—mode

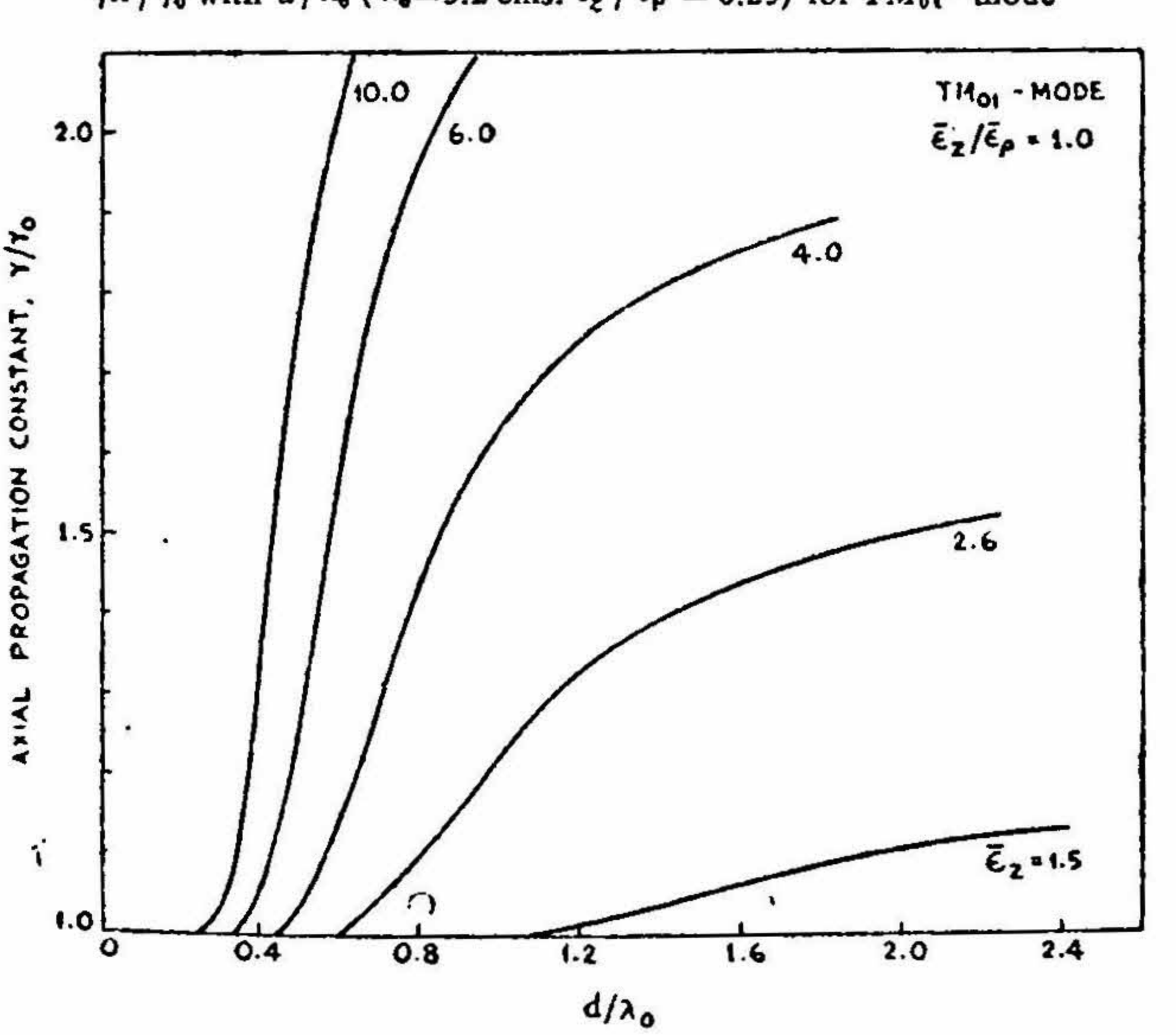

FIG. XIX

Variation of the axial propagation constant,
$\gamma H / \gamma_0$ with d/λ_0 (λ_0=3.2 cms. $\bar{e}_z / \bar{\epsilon}_\rho$ =1.0) for TM_{01}—mode

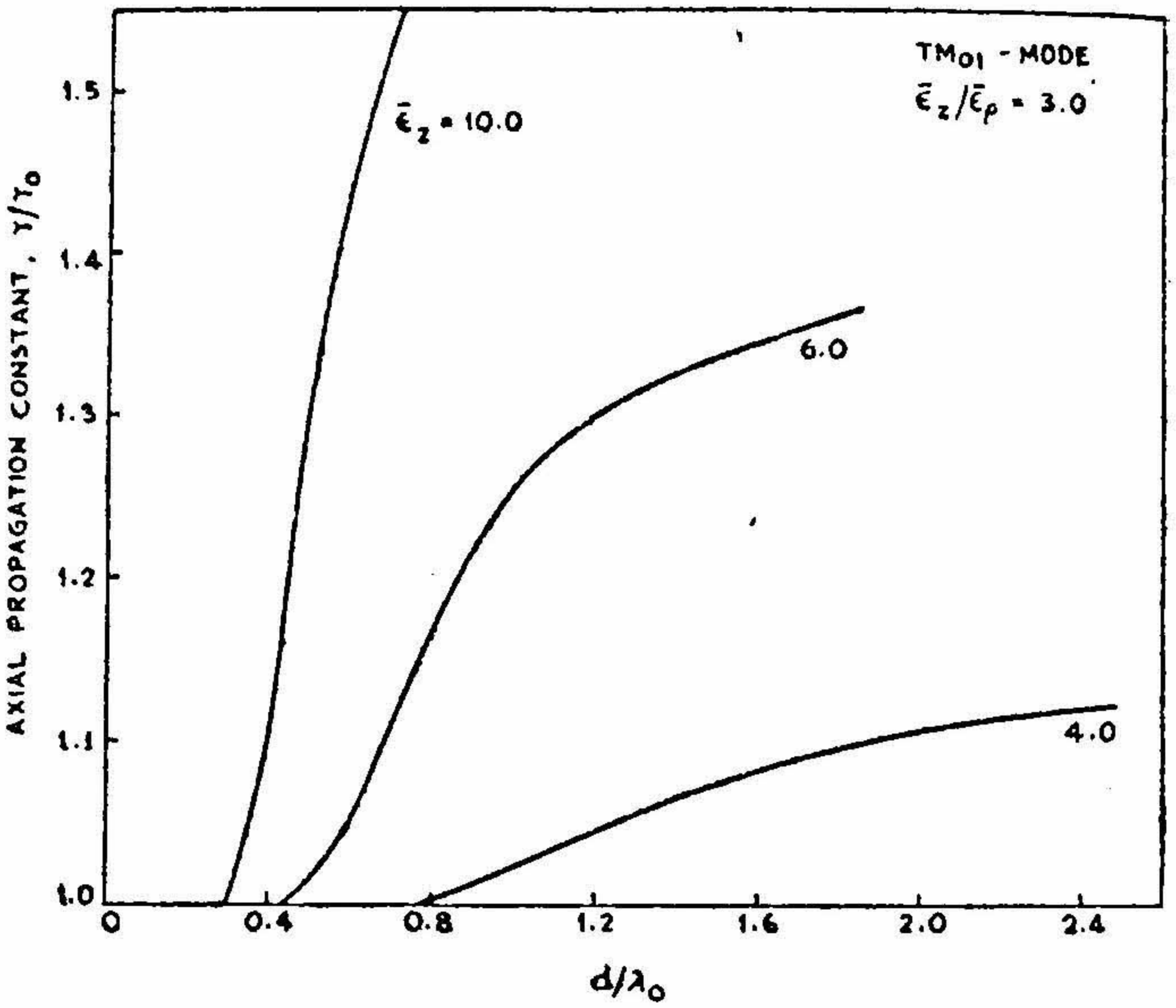

FIG. XX

Variation of the axial propagation constant, γ^H/γ_0 with d/λ_0 (λ_0=3.2 cms. $\bar{\epsilon}_z/\bar{\epsilon}_\rho$ = 3.0) for TM_{01}—mode

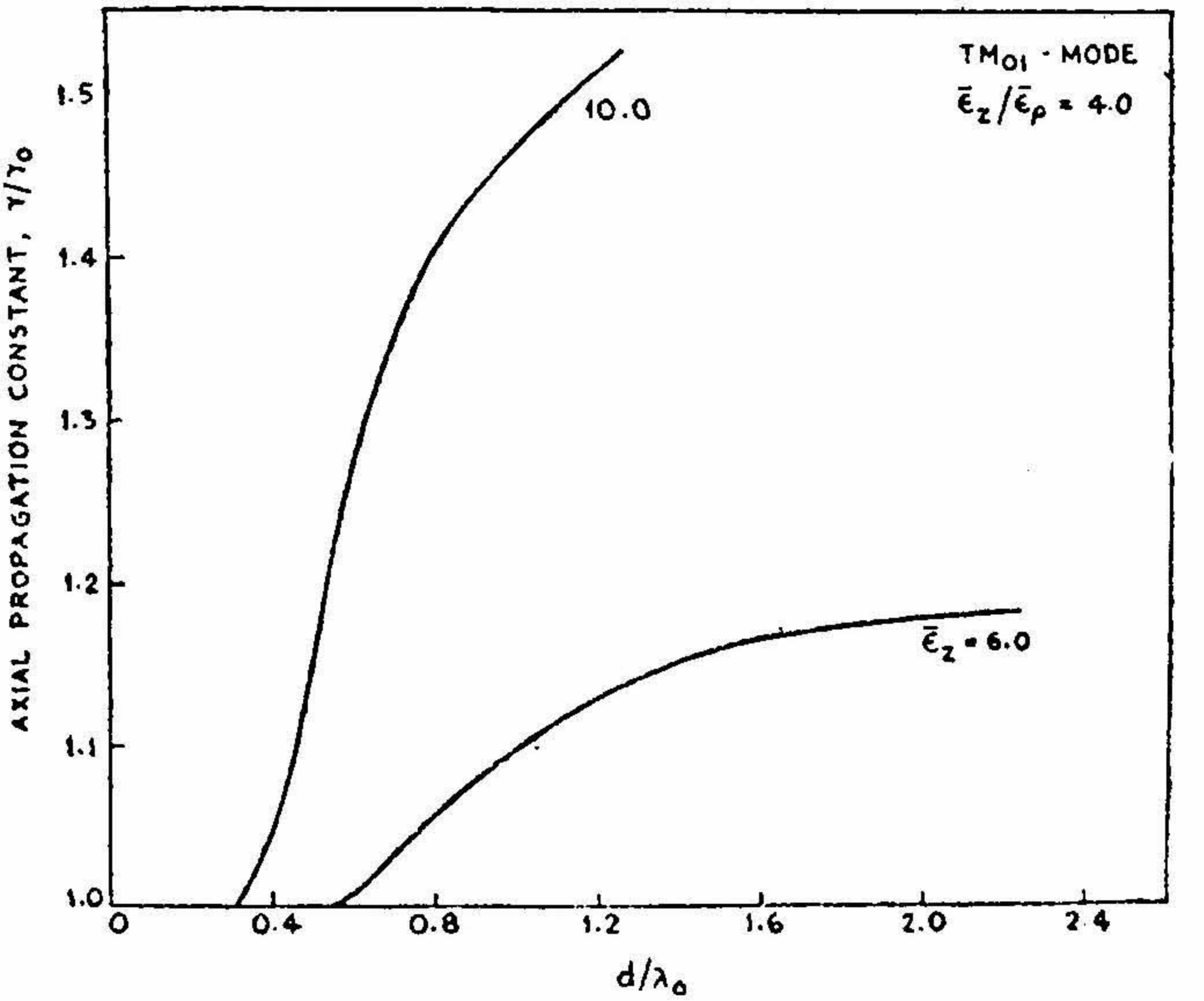

FIG. XXI

Variation of the axial propagation constant, γ^H/γ_0 with d/λ_0 (λ_0=3.2 cms. $\bar{\epsilon}_z/\bar{\epsilon}_\rho$ = 4.0) for TM_{01}—mode

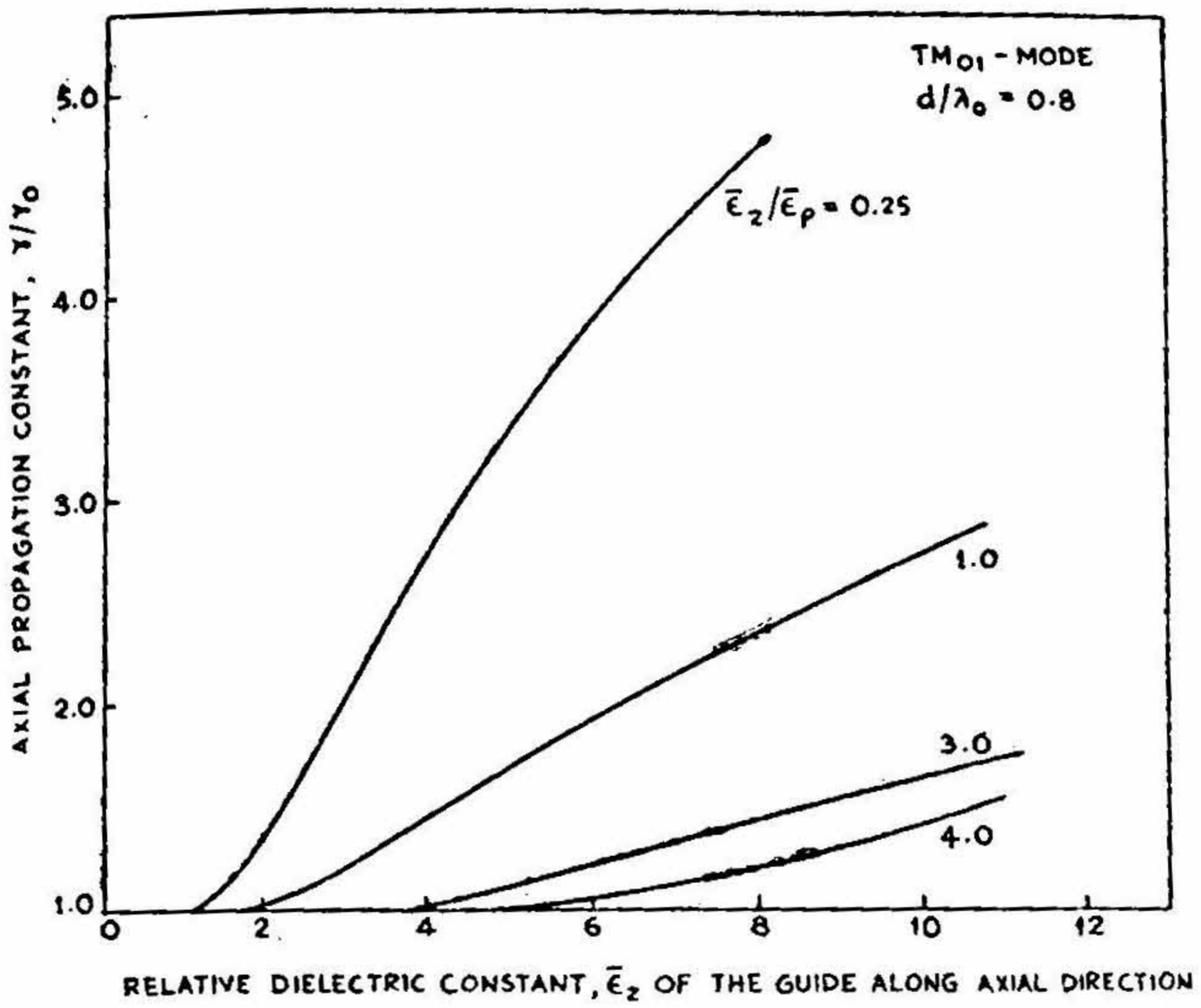

FIG. XXII

Variation of the axial propagation constant, γ^H/γ_0 with $\bar{\epsilon}_z$ ($d/\lambda_0=0.8$, $\lambda_0=3.2$ cms.) for TM_{01}—mode

4.5 *Cut-off Conditions*

It is seen from the solutions of the characteristic equations [10], [12], [13] and [14] that for the axially symmetric modes, propagation along the guide is not possible without radial loss of energy for waveguide diameters less than a limiting diameter and for wavelengths greater than a corresponding limiting wavelength depending on the dielectric constants and the permittivities of the medium. This is the cut-off phenomenon for these modes. Immediately above this limiting value, $\lambda_g \approx \lambda_0$ and only a smaller part of the energy flows inside the guide.

For values of (d/λ_0) greater than the limiting value, the guided wavelength becomes smaller and smaller and approaches $[\lambda_0 (\bar{\epsilon}_\rho)^{-\frac{1}{2}}]$ and power flow tends rapidly to be confined totally within the rod. Or, in other words, at $(\lambda_g/\lambda_0) \geq 1$ and with real arguments of Hankel functions, solution of the characteristic equation yields a minimum value of (d/λ_0), which we define as the condition of cut-off. They are given as,

$$(d/\lambda_0)_{\text{cut-off}} = \begin{cases} \dfrac{S_n}{\pi}\left[\bar{\epsilon}_z - (\bar{\epsilon}_z/\bar{\epsilon}_\rho)\right]^{-\frac{1}{2}} & \text{for } TM_{0n} \text{ waves} \\ \dfrac{S_n}{\pi}\left[\bar{\epsilon}_\rho - 1\right]^{-\frac{1}{2}} & \text{for } TE_{0n} \text{ waves} \end{cases}$$

where, S_n = value of the argument of $J_0(x)$ for $J_0'(x) = 0$ and, $n = 1, 2, 3, 4$ . . . indicating dominant and higher order mode configurations.

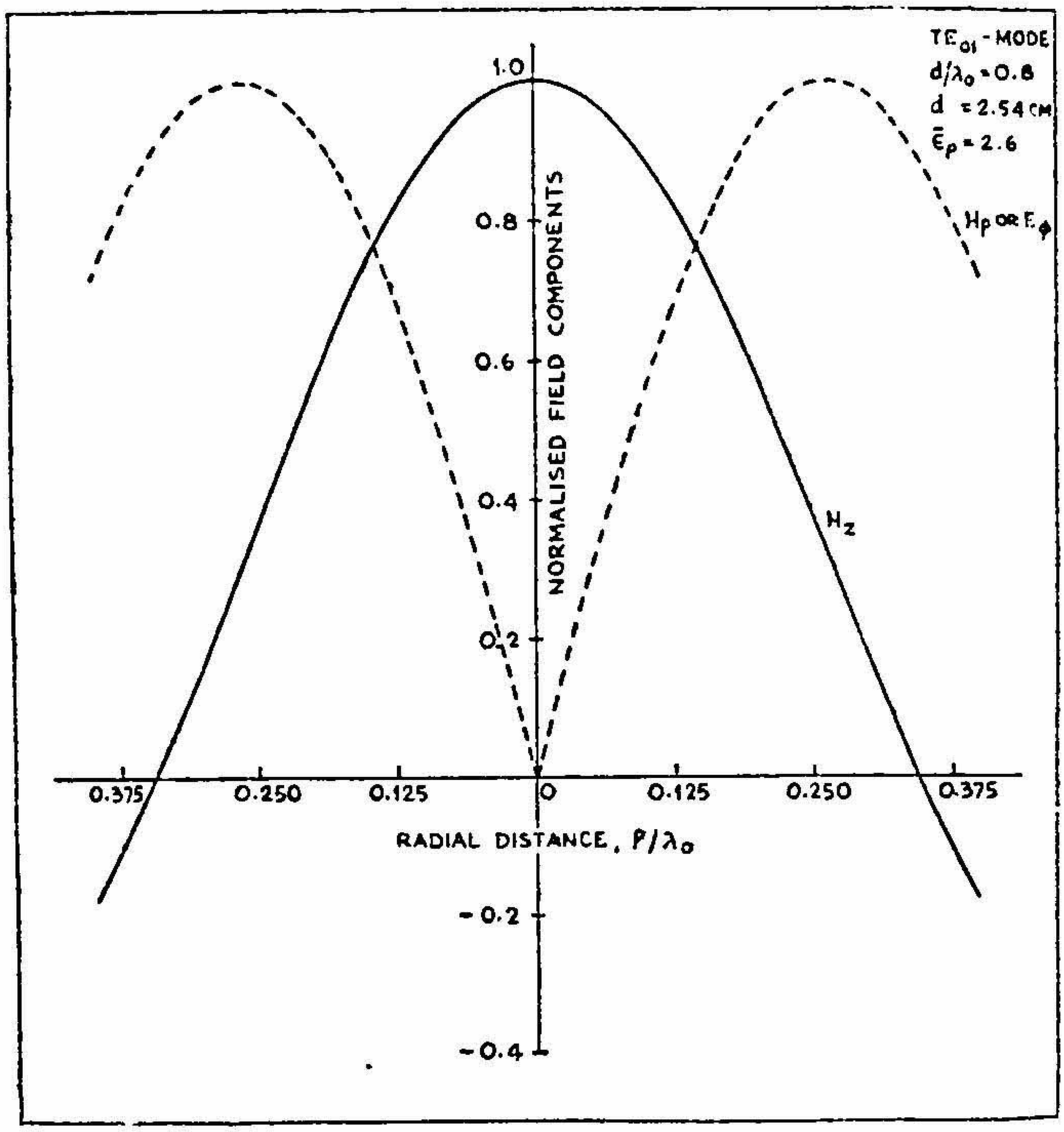

FIG. XXIII

Variation of the field components, H_z, E_ϕ, H_ρ, with the radial distance, ρ/λ_0, inside the guide for TE_{01}—mode. ($\bar{\epsilon}_\rho = 2.6$, $d/\lambda_0 = 0.8$, $\lambda_0 = 3.2$ cms.) (E_ϕ, $H\rho$: have been normalised with respect to their values E'_ϕ and H'_ρ, respectively, at $\rho = 0.8$ cms.)

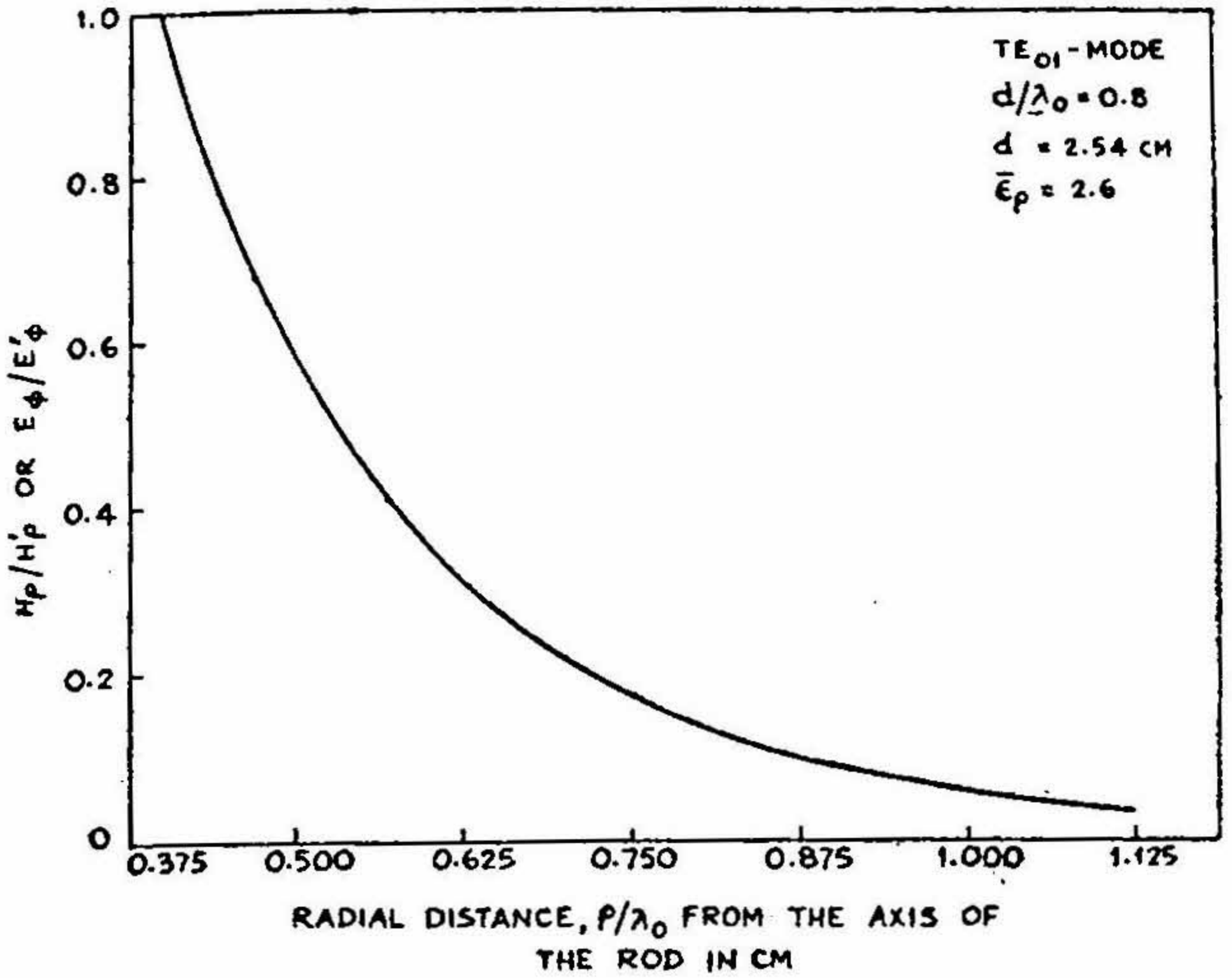

FIG. XXIV

Variation of the field components, H_ρ, H_ϕ with the radial distance, ρ/λ_0, outside the guide for TE_{01} mode ($\bar{\epsilon}_\rho = 2.6$, $d/\lambda_0 = 0.8$, $\lambda_0 = 3.2$ cms.) (H_ρ, E_ϕ have been normalised with respect to their vales H'_ρ and E'_ϕ, respectively on the surface of waveguide, $\rho = r$)

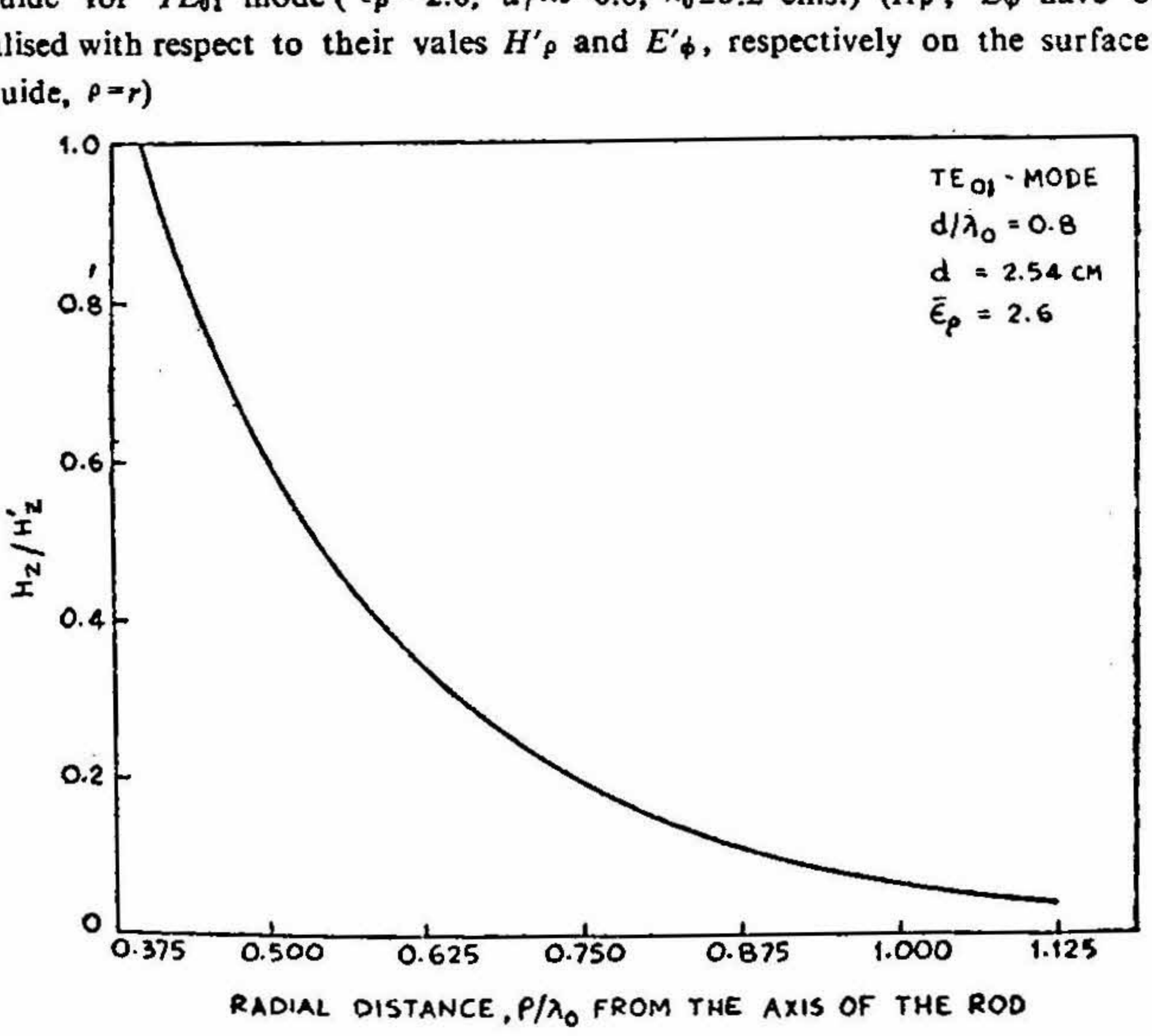

FIG. XXV

Variation of the field component H_z with the radial distance ρ/λ_0 outside guide for TE_{01} mode ($\bar{\epsilon}_\rho = 2.6$, $d/\lambda_0 = 0.8$, $\lambda_0 = 3.2$ cms.) (H_z has been normalised with respect to its value. H'_z at the surface of the waveguide, $\rho = r$)

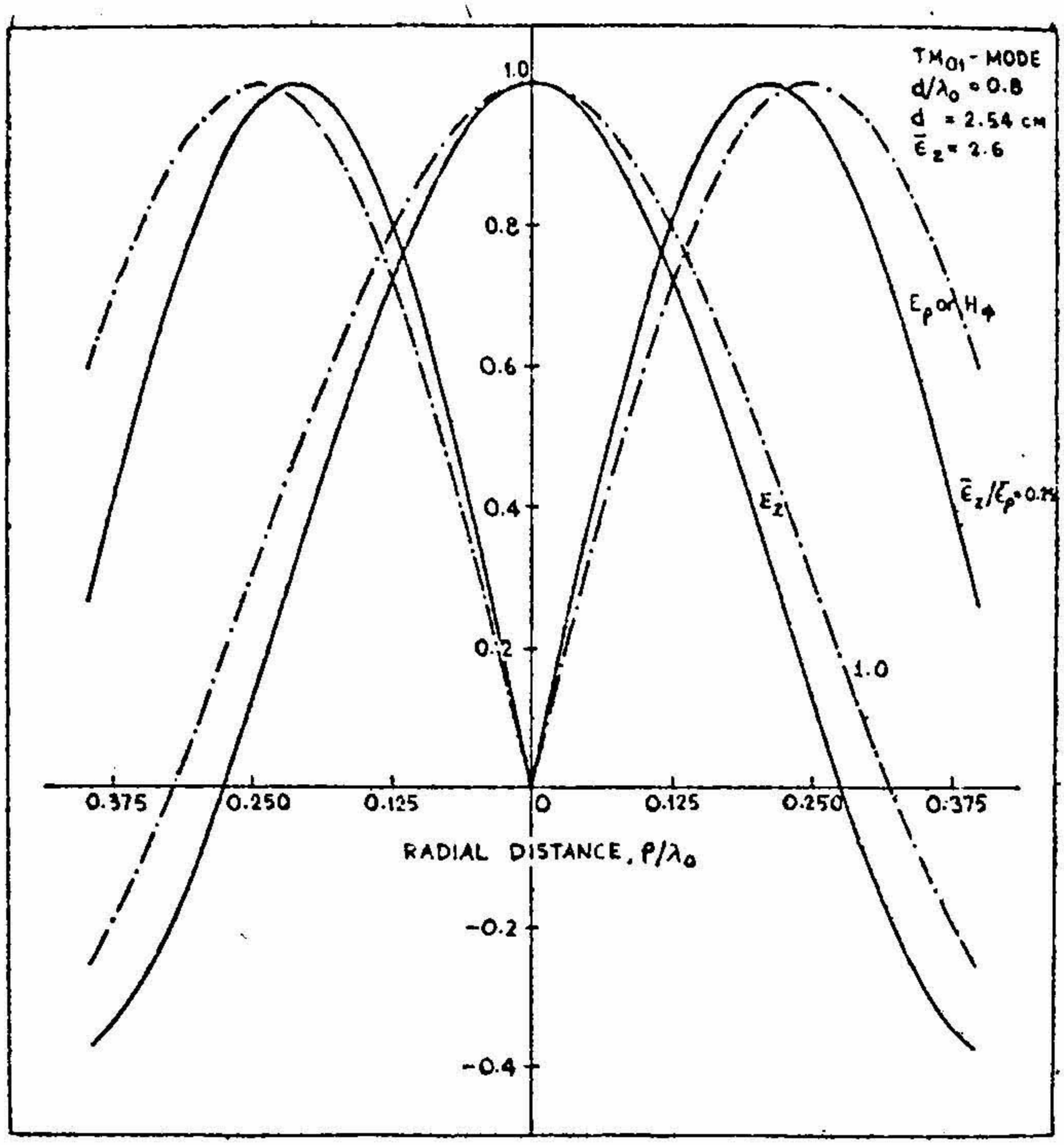

FIG. XXVI

Tariation of the field components, E_z, E_ρ, H_ϕ with the radial distance, ρ/λ_0, inside the guide for TM_{01} mode ($\bar{\epsilon}_z = 2.6$, $d/\lambda_0 = 0.8$, $\lambda_0 = 3.2$ cms: $\bar{\epsilon}_z / \bar{\epsilon}_\rho = 2.5, 1.0$) ($E_\rho$, H_ϕ have been normalised with respect to their values, E'_ρ and H'_ϕ respectively, at $\rho = 0.675$ cms, 0.7853 cms. for the two different $\bar{\epsilon}_z / \bar{\epsilon}_\rho$.)

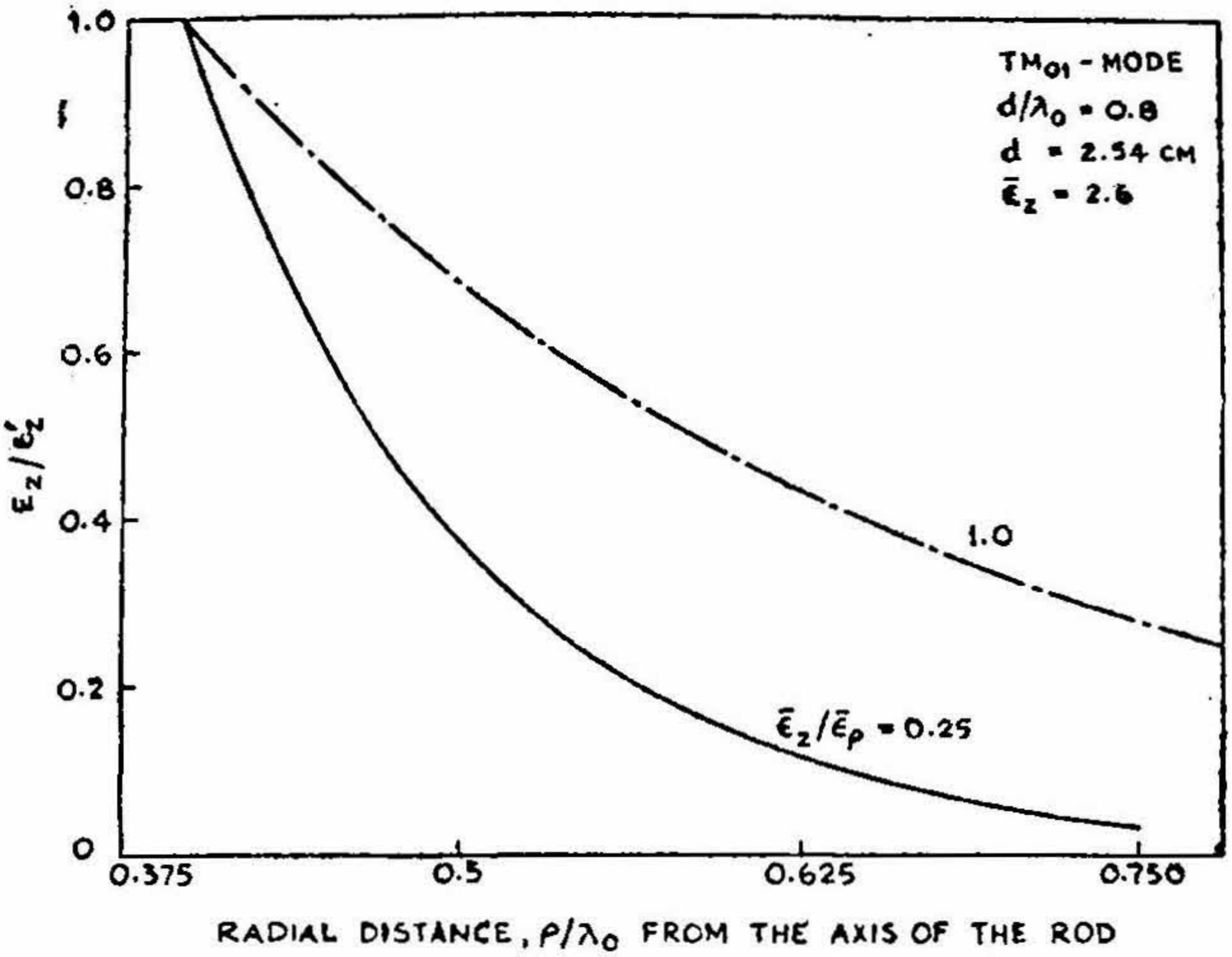

FIG. XXVII

Variation of the fieid component, E_z with the radial distance, ρ/λ_0 outside the guide for TM_{01}—mode ($\bar{\epsilon}_z = 2.6$, $d/\lambda_0 = 0.8$, $\lambda_0 = 3.2$ cms, $\bar{\epsilon}_z/\bar{\epsilon}_\rho = 0.25, 1.0$) E_z has been normalised with respect to its value E'_z on the surface of the waveguide, $\rho = r$).

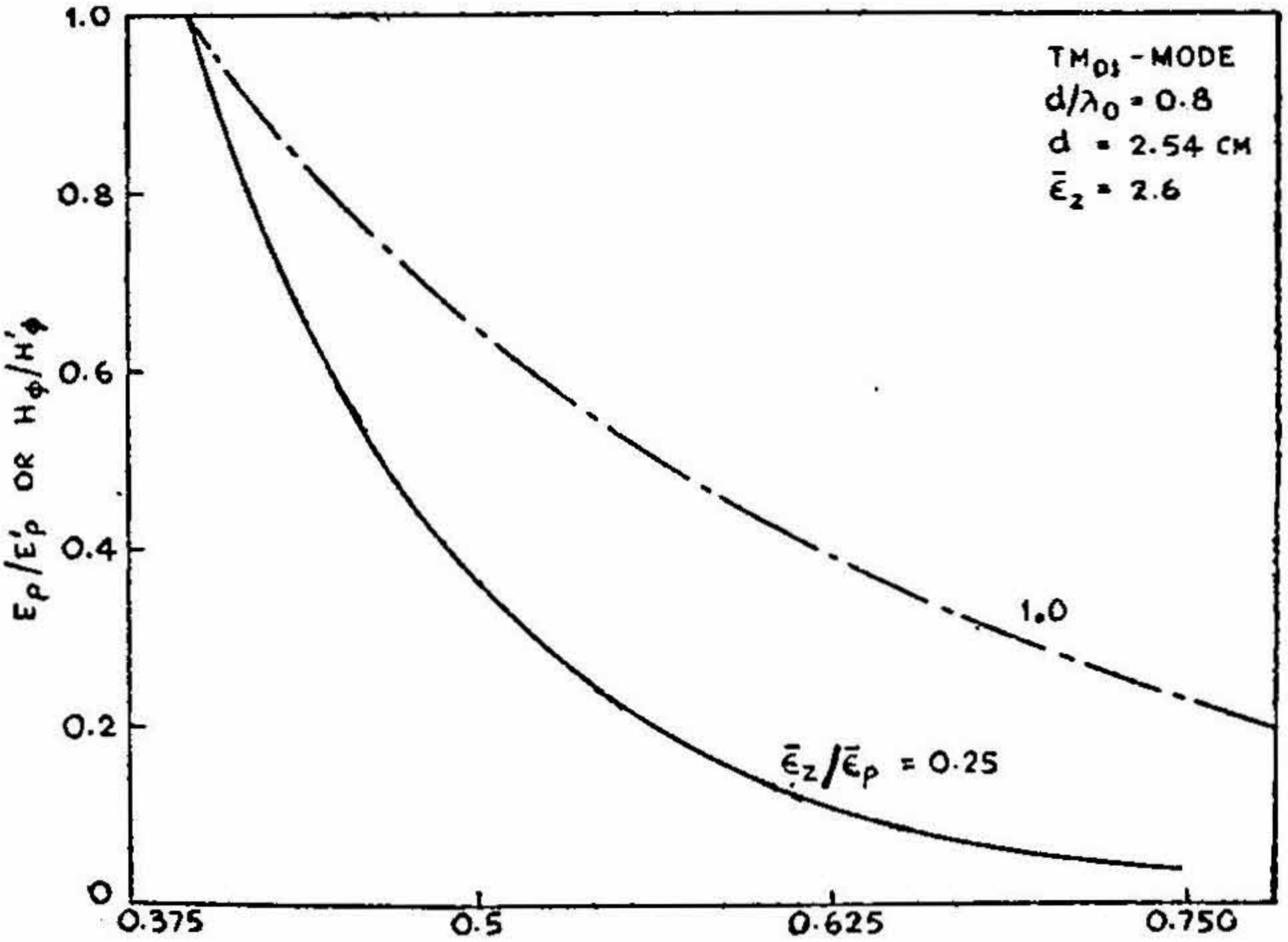

FIG XXVIII

Variation of the field components, E_ρ , H_ϕ with the radial distance, ρ/λ_0, outside the guide for TM_{01}—mode ($\bar{\epsilon}_z = 2.6$, $d/\lambda_0 = 0.8$, $\lambda_0 = 3.2$ cms, $\bar{\epsilon}_z/\bar{\epsilon}_\rho = 0.25$, 1.0 ($E_\rho$, H_ϕ have been normalised with respect to their values E'_ρ , H'_ϕ , respectively on the surface of the guide, $\rho = r$ for the two different $\epsilon_z/\bar{\epsilon}_\rho$).

For dominant modes, $S_{11} = 2.405$ and cut-off conditions are plotted as a function of $\bar{\epsilon}_\rho$ for TE_{01} mode and as a function of $\bar{\epsilon}_2$ with $[\bar{\epsilon}_z/\bar{\epsilon}_\rho]$ ranging from 0.25 to 4.0 for TM_{01} mode in the Figures XXIX and XXX, respectively.

5. CONCLUSION

It is observed from the graphs of the guided-wavelength that λ_g decreases with an increase in the dielectric constants, $\bar{\epsilon}_z$, $\bar{\epsilon}_\rho$. The decrease of λ_g with an increase in the diameter of the guide may be due to the increase in the axial propagation constant, as an increase in $\gamma = i\beta$, for a loss-less waveguide, reduces the phase velocity of the propagating wave. In the case of *TM*-waves, λ_g increases with an increase of $[\bar{\epsilon}_z/\bar{\epsilon}_\rho]$ for any $\bar{\epsilon}_z$.

From the curves of radial and axial propagation constants it will be seen that K_1 decreases and K_2 and γ increase with larger diameter of the guide, and with an increase in the diclectric constants, $\bar{\epsilon}_z$, $\bar{\epsilon}_\rho$ all the three constants, K_1, K_2 and γ increase. However, the rate of increase of K_1 with increase of dielectric constants is less compared to those of K_2 and γ. This accounts for the reduction in the radial-field spread for such wave-guides having larger diameters and higher dielectric constants.

It will be evident from equation (3) that on substituting $[\bar{\epsilon}_z/\bar{\epsilon}_\rho] = 1$, the propagation characteristics for TM_{01} mode in an isotropic dielectric rod wave-guide (Kiely, 1953) are obtained. For the TE_{01} mode, however, the solutions

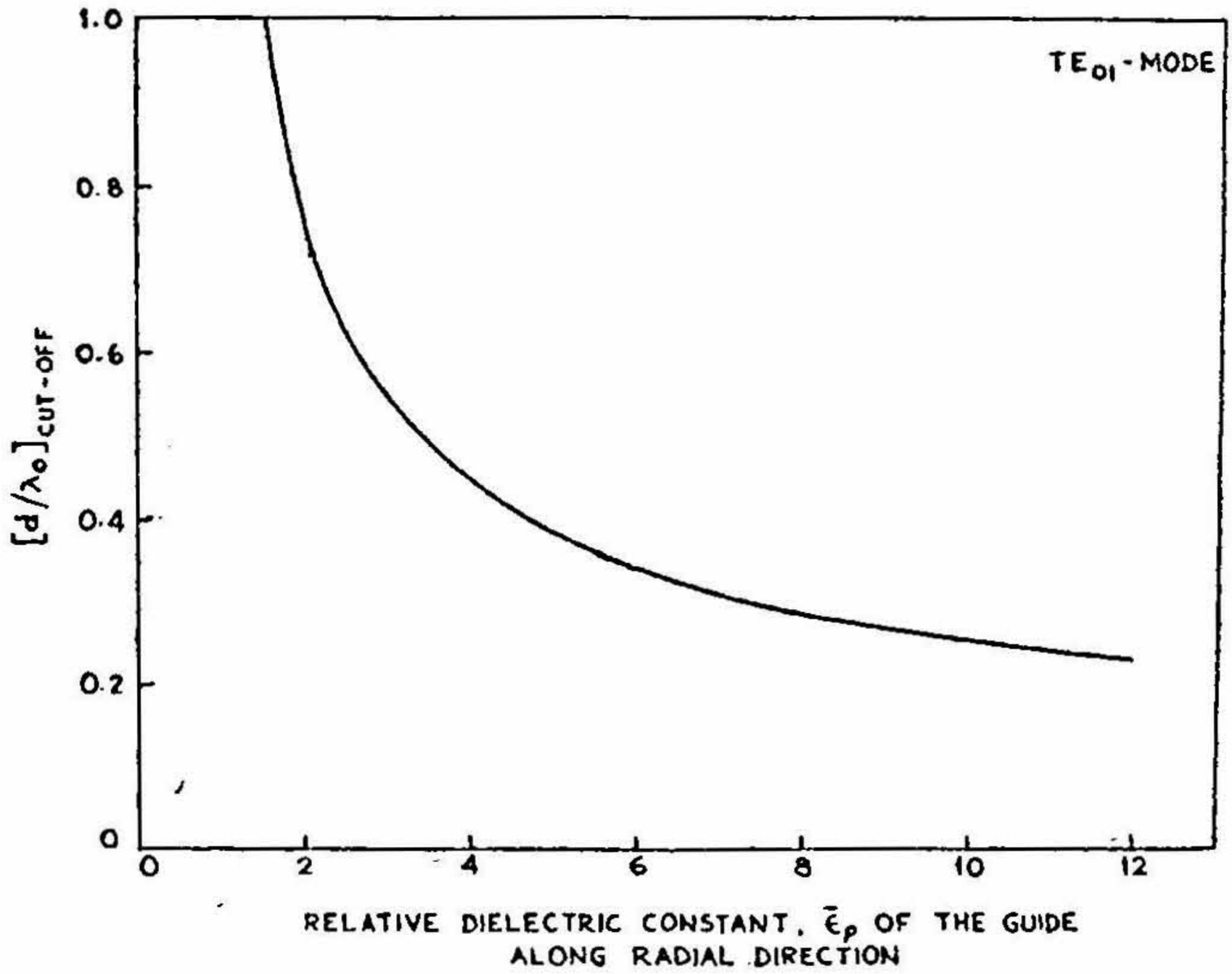

FIG. XXIX

Variation of the cutoff condition, (d/λ_0) cutoff with $\bar{\epsilon}_\rho$ ($\lambda_0 = 3.2$ cms.) for TE_{01}—mode.

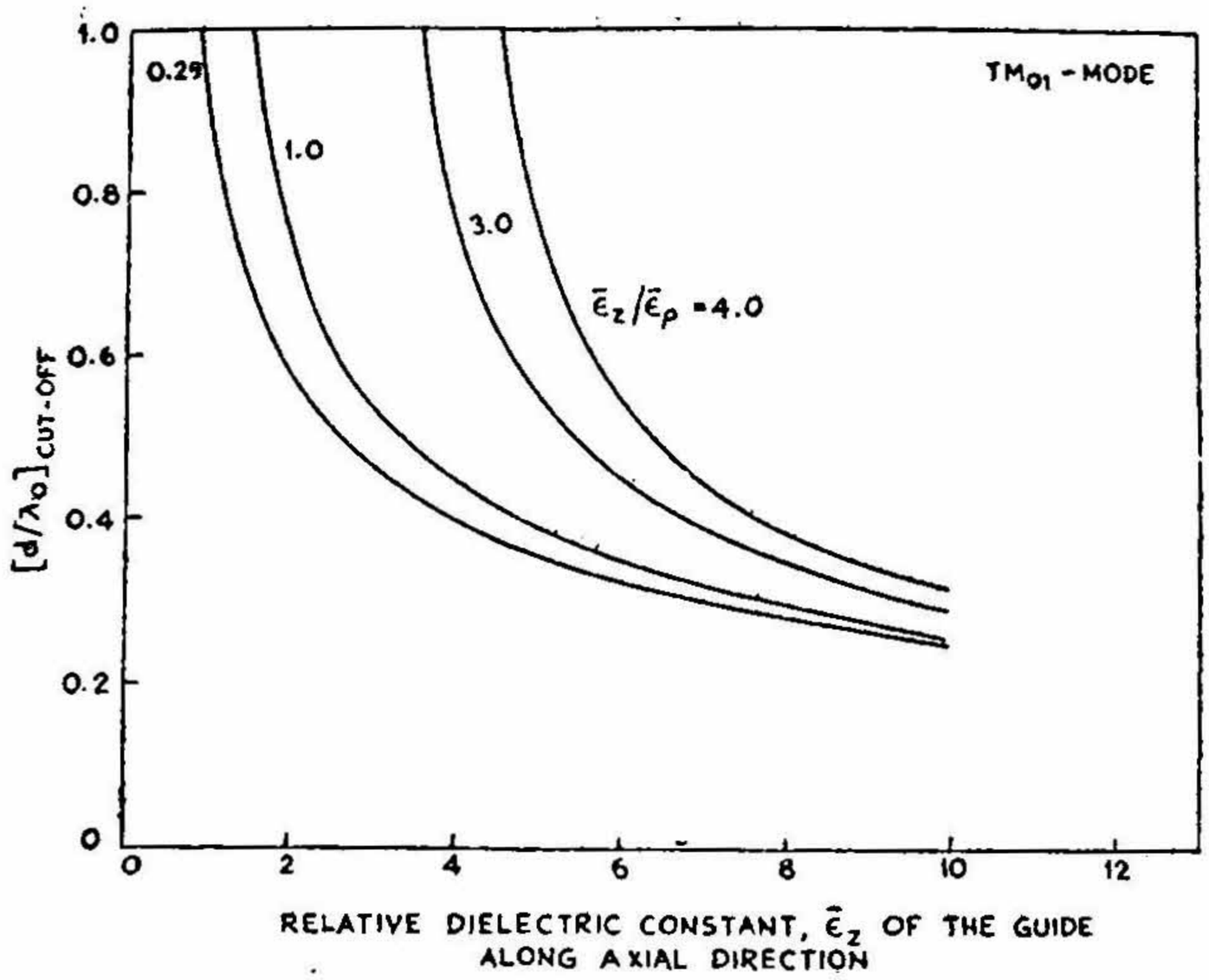

FIG. XXX

Variation of the cutoff condition, (d/λ_0) cutoff with $\bar{\epsilon}_z$ (λ_0= 3.2 cms. for TM_{01}—mode.

are similar to those for the isotropic wave-guides as $\bar{\epsilon}_\rho$ only is involved due to the nature of the field configurations.

For the circularly symmetrical TM_{01} mode and $(d/\lambda_0) = 0.8$, $\bar{\epsilon}_z = 6.0$, the propagation characteristics of surface waves through an isotropic dielectric rod waveguide have been compared with those for an isotropic dielectric rod guide in Table I.

TABLE I

Comparative Study of the Propagation Characteristics

$[\bar{\epsilon}_z/\bar{\epsilon}_\rho]$	0.25	1.0	3.0	4.0
$[\lambda_g/\lambda_0]$	0.258	0.511	0 810	0.943
K_1^H	2.95	2 89	2.71	2.47
K_2^H/i	7.39	3.32	1.37	0.697
$[\gamma/\gamma_0]$	3 83	1.93	1.22	1.04
$[d/\lambda_0]$ cutoff	0 320	0.347	0.443	0.544

From the above it is quite clear that for any anisotropic dielectric rod waveguide, the fields get more and more concentrated inside the guide with decreasing anisotropicity, *i.e.*, $\left[\frac{\bar{\epsilon}_z}{\bar{\epsilon}_\rho}\right]$ tending to lower values. This results into the relative advantages over its isotropic counterpart in transmitting power over a longer distance along the guide.

ACKNOWLEDGEMENTS

The author expresses his thanks to Mr. S. K. Chatterjee, for the guidance and some helpful discussions about this work. He acknowledges his gratitude to Professor S. V. C. Aiya, for the encouragement and the facilities provided during the course of the work. Acknowledgements are also due to the University Grants Commission for the award of a Senior Research Fellowship.

REFERENCES

1. Barlow, H. E. M. and Brown, J. — Radio Surface Waves, International Monographs on Radio, (Oxford University), 1962.
2. ——— and Karbowiak, A. E. — Proceedings of the Institution of Engineers, 1954, 101, Part 3, 182.
3. Colin, R. .. .. — Field Theory of guided waves, (McGraw Hill, U. S. A.), 1958.
4. Kiely, D. G. .. .. — Dielectric Aerials, Methuen, Monographs (John Wiley and Sons, Inc., N. Y.), 1953.
5. Lines, A. W. and Nicoll, G. R. .. — British Telecommunication Research Establishment Report, No. T, 1948, 2114.
6. Mueller, G. E. .. .. — Proceedings of the Institution of Radio Engineers, N. Y., 1952, 40, 71.
7. Paul, D. K. .. .. — *Electrotechnics*, 1963, 29, 53.
8. Piefke, G. .. .. — Institution of Radio Engineers Transaction on Antenna and Propagation, Special Supplement, 1959, AP—7, S. 183.
9. Simon, J. C. and Weill, G. .. — *C. R. del Academic des Sciences*, 1952, 235, 1379.
10. Subrahmaniam, V. .. .. — *J. Indian Inst. Sci.* 1962, 44, 148.
11. Subrahmaniam, V. .. .. — *Ibid* 1963, 45, 109.

LIST OF SYMBOLS

E	Electric field vector.
H	Magnetic field vector.
μ	Permeability of the outer medium, air.
ϵ	Dielectric constant of the outer medium, air.
ϵ_1	Dielectric constant of the anisotropic dielectric rod.

ϵ_ρ	Tensor component of ϵ_1 in the radial direction.
ϵ_z	Tensor component of ϵ_1 in the longitudinal direction.
γ_1^E, γ_2^E	Axial propagation constants inside and outside the waveguide respectively, for TE_{01} mode.
γ_1^H, γ_2^H	Axial propagation constants inside and outside the waveguide respectively, for TM_{01} mode.
λ_g	Guided wave-length, cm.
λ_0	Wavelength in free-space, 3.2 cm.
d	Diameter of the waveguide, cm.
K_1^E, K_2^E	Radial propagation constants inside and outside the waveguide respectively, for TE_{01} mode.
K_1^H, K_2^H	Radial propagation constants inside and outside the waveguide respectively, for TM_{01} mode.
A, B, C, D	Constants to be determined from boundary conditions.
$J_0(x)$, $H_0^{(1)}(x)$	Zero-order Bessel and Hankel functions of the first kind, respectively.
$J_1(x)$, $H_1^{(1)}(x)$	First-order Bessel and Hankel functions of the first kind, respectively.